As originally published in the SMTA Proceedings.

PERM DoD Consortium Phase 3 Pb-free Solder Thermal Cycle Reliability Results Comparing Different Levels of Bismuth Alloying

Tim Pearson, David Hillman, Ross Wilcoxon,
Julie Mills, Leela Herena
Collins Aerospace
IA, USA
Timothy. J. Pearson@collins.com

ABSTRACT
Pb-free soldering processes and materials have been implemented in the commercial electronics sector due to the European Union Waste Electrical and Electronic Equipment (WEEE) and Reduction of Hazardous Waste (RoHS) Directives. These environmental legislative directives were targeted at industrial and commercial electronic products but had an unintended impact on aerospace/defense products due to global supply chain transition actions. A group of industry, academic, and government agencies initiated a Pb-free solder alloy reliability investigation, building on previous activities, to characterize and understand various aspects of Pb-free solder joint integrity under -55°C to +125°C thermal cycle conditions. The goal of the testing was to generate reliability data for test vehicles that were representative of IPC Class III High Performance Electronic products.

Key words: Pb-free alloys, high-reliability solder alloys, thermal fatigue reliability, failure mode, solid solution strengthening.

INTRODUCTION

Collins Aerospace has been a primary participant in the IPC Pb-free Electronics Risk Management (PERM) DoD Phase 3 industry consortium effort to understand Pb-free soldering materials and processes. This paper documents the Collins Aerospace thermal cycle testing effort for the IPC PERM DoD consortium program. The IPC PERM DoD Phase 3 consortium is a continuation of the Joint Council on Aging Aircraft/Joint Group on Pollution Prevention (JCAA/JG-PP) Pb-free Solder Project [1], an established industry consortium project focused on evaluating the reliability of Pb-free solder alloys for the requirements of the aerospace and military electronics products, and the NASA DoD Phase 2 Project [2].

Solder Alloy Testing Background

The following solder alloys for testing were selected for testing in the JCAA/JGPP Pb-free Solder Project investigation:

- **Sn3.9Ag0.6Cu** (SAC) for reflow and wave soldering (SAC396: Tin (Sn); Silver (Ag); Copper (Cu))
- **Sn3.4Agl.00u3.3Bi** (SACB) for reflow soldering (SACB: Tin (Sn); Silver (Ag); Copper (Cu); Bismuth (Bi))
- **Sn0.7Cu0.05Ni** (SN100C) for wave soldering (SN100C: Tin (Sn); Copper (Cu); Nickel (Ni); Germanium (Ge))
- **Sn37Pb** (SnPb) for reflow and wave soldering

The following solder alloys were selected for testing in the NASA DoD Pb-free Phase 2 Project investigation:

- **Sn3.0Ag0.5Cu** for reflow and manual soldering (SAC305: Tin (Sn); Silver (Ag); Copper (Cu))
- **Sn0.7Cu0.05Ni** for reflow, wave, and manual soldering (SN100C: Tin (Sn); Copper (Cu); Nickel (Ni); Germanium (Ge))
- **Sn37Pb** (SnPb) for reflow, wave, and manual soldering

Several ternary tin-silver-bismuth (SnAgBi) and quaternary tin-silver-copper-bismuth (SnAgCuBi) Pb-free solder alloys demonstrated improved mechanical and thermo-mechanical reliability in the aforementioned projects [3]. For the IPC/PERM DoD Phase 3 Pb-free Project investigation, the solder alloys selected for testing were revised to include SACBi alloys, due to emerging interest in these alloys in the electronics industry. The Sn63Pb37 solder alloy was again included for a baseline comparison.

The following solder alloys were selected for testing in the IPC/PERM DoD Pb-free Phase 3 Project investigation:

- **Sn63Pb37** (SnPb)
- **Sn3.0Ag0.5Cu** (SAC305)
- **Sn3.4Ag4.8Bi** (SAC4.8Bi)
- **Sn2.25Ag0.5Cu6.0Bi** (SAC6.0Bi)
- **Sn2.0Ag7.5Bi** (SAC7.5Bi)

Test Vehicle

The test vehicle used for the thermal cycle testing was the same circuit design used in the NASA DoD Phase 2 project. The circuit board was 11.5 inches by 9.5 inches by 0.080 inches thick and contained 6 layers of 0.5 ounce copper. The test vehicle was designed to meet IPC-6012, Class 3, Type 3 requirements. Two printed circuit board laminate materials were included in the investigation: Isola 408HR and Isola 370HR. The laminates were FR4 per IPC-4101/26 with a minimum Tg of 170°C. The majority of the test vehicles used an immersion silver (ImAg) finish and a small set of test boards with Isola 408HR laminate used an electroless nickel/immersion gold (ENIG) surface finish. The Isola 370HR laminate was used in the previous investigation test vehicles, thus enabling "apples-to-apples" data comparisons. A total of 30 test vehicles were thermal cycled for this study. Figure 1 illustrates the circuit board construction.

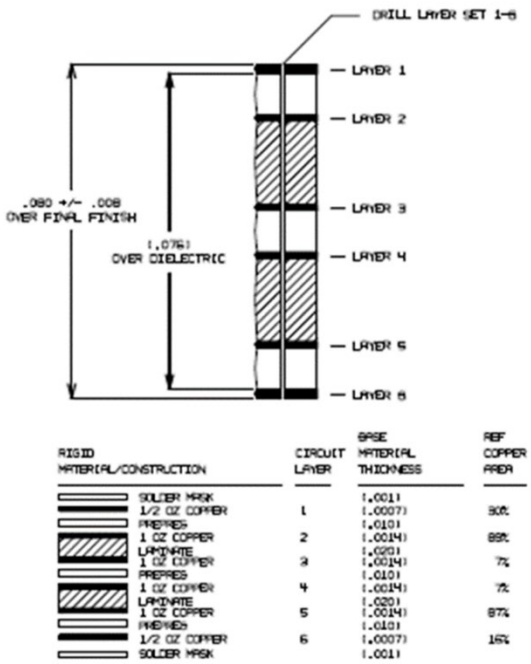

Figure 1: Test Vehicle Design

Test Components

A variety of component types were included in the investigation. The PBGAs, MLF, CLCC, and TQFP components (see Table 1 for acronym definitions) were used on the previous investigation test vehicles, thus enabling "apples-to-apples" data comparisons to prior data sets. The LGA and SOT-23 components were added by the investigation team to accumulate solder joint integrity data that was not readily available in the published literature. The POP components were included for the same reason, but not used on the test vehicle due to a component footprint layout error. All components except the LGA were procured from Practical Components. The LGA component was procured from Linear Tech. Table 1 lists the various component types and their surface finishes.

Table 1 Investigation Component Information

Component	Size, mm	Pitch, mm	# I/O	Lead Finish/ Alloy
PBGA	35 x 35	1	1156	SnPb and SAC305
PBGA	27 x 27	1	676	
MLF	5 x 5	0.65	20	SnPb and Sn
CLCC	8.9 x 8.9	1.27	20	Au (pre-tinned SnPb and SAC305)
TQFP	22 x 22	0.5	144	Sn
LGA	9 x 11	1.27	50	Au
SOT-23	2.4 x 2.9	1.9	3	Sn
POP	12 x 12	0.65	128	SAC305
Plastic Ball Grid Array (PBCA), Micro Lead Frame (MLF), Ceramic Leadless Chip Carrier (CLCC), Thin Quad Flatpack (TQFP), Land Grid Array (LGA), Small Outline Package (SOT-23), Package on Package (POP)				

The test vehicle components are representative of components used in military/aerospace systems and selected to reveal relative differences in solder alloy performance. The CLCC component was chosen due to industry recognized solder joint integrity issues in Class III High Performance electronic products. The CLCCs were pre-tinned by an external service provider with both SnPb and SAC305 solders to eliminate the issue of gold embrittlement. The TQFPs and PBGAs were selected to represent leaded and leadless surface mount technologies. Appendix E provides detailed component mechanical information.

Test Vehicle Assembly

The test vehicles were assembled at the Collins Aerospace Coralville, Iowa facility. Standard surface mount technology (SMT) automated reflow SnPb and Pb-free soldering processes were used. All assembled test vehicles were inspected and found to be acceptable per the IPC-JSTD-001/IPC-A-610 specification set. Figure 2 illustrates a fully assembled and chamber-ready test vehicle.

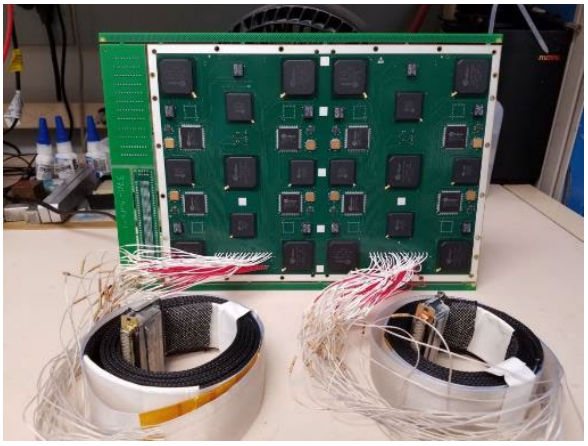

Figure 2: Assembled Test Vehicle Wired for Thermal Cycle Testing

Thermal Cycle Parameters and Methodology

The temperature cycle range used for the testing was -55°C to +125°C with 10-minute dwells at the temperature extremes. A maximum temperature ramp of 10°C/minute was used in the testing. The continuity of the component solder joints was continuously monitored throughout thermal cycle testing by an event detector, in accordance with the IPC-9701 specification, with each component treated as a single resistance channel. An 'event' was recorded if the resistance of a channel exceeded 300 Ω for more than 0.2 µsec. A failure was defined when a component either:

- Recorded an event for 15 consecutive cycles,
- Had five consecutive detection events within 10% of current life of test, or
- Became electrically open

Once a solder joint was designated a failure, the event detection system software excluded it from the remainder of the test. Detailed temperature profiling was conducted prior to the beginning of the thermal cycle conditioning to ensure that each test vehicle was subjected to uniform, consistent exposure to the test chamber temperatures. Figure 3 illustrates measured test vehicle temperatures for testing done

with the -55°C to +125°C thermal cycle temperature profile. Figure 4 illustrates the test vehicles positioned in the test chamber. The aluminum foil visible in Figure 4 served as part of the air baffle system for uniform heating of test vehicles.

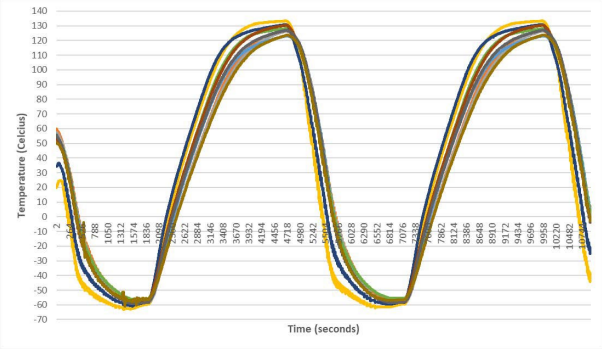

Figure 3: Test vehicle temperatures during -55C to +125C thermal cycling

Figure 4: Test vehicles positioned in the thermal cycle chamber

Test Results

The -55°C to +125°C thermal cycle testing was terminated after 4362 total thermal cycles. The physical failure and statistical analysis for each component type are summarized in the following sections for each specific component style. It should be noted that the test vehicles remained in the thermal cycle chamber the entire 4362 cycles. Individual components were left in the test chamber after they had failed to prevent potentially damaging the solder joints of other components on the test vehicles through handling/movement. This resulted in some continuing solder joint microstructure evolution after the initial component failure, which is evident in some of the physical failure analysis pictures. The data in the following summaries does not include thermal cycle results that showed a failure before 1 cycle, unless otherwise stated. These early failures were reviewed and discounted due to assignable root cause (i.e., a manufacturing problem) or event detector wire connections. Table 2 shows the failure rates of each component by alloy at the end of 4362 thermal cycles.

Table 2: Component Population Failure Rates after 4362 Thermal Cycles

	SnPb	SAC305	SAC 4.8Bi	SAC 6.0Bi	SAC 7.5Bi
PBGA-1156	24%	10%	5%	12%	7%
PBGA-676	100%	77%	33%	17%	27%
MLF-20	8%	100%	88%	98%	81%
LGA	38%	10%	3%	12%	5%
SOT-23	71%	67%	21%	13%	38%
CLCC-20	98%	98%	100%	100%	100%
TQFP-144	94%	100%	83%	73%	75%

Plastic Ball Grid Array (PBGA-1156) Results

Statistical Analysis

The PBGA-1156 components accumulated an overall 11.4% population failure after the completion of 4362 thermal cycles. SnPb had the highest failure rate at 23.7% failure, while SAC4.8Bi and SAC7.5Bi had the lowest at 5.0% and 6.7% respectively. While all the alloys had low failure rates, the Pb-free alloys performed better than SnPb. Figure 5 and Figure 6 summarize the PBGA-1156 thermal cycle test results. Figure 5 shows results for all failures that occurred after at least one thermal cycle while Figure 6 only shows data for failures that occurred after 500 cycles. This filtering was applied to the data to remove the effects of infant mortality so that the long-term reliability trends for the overall populations could be better understood.

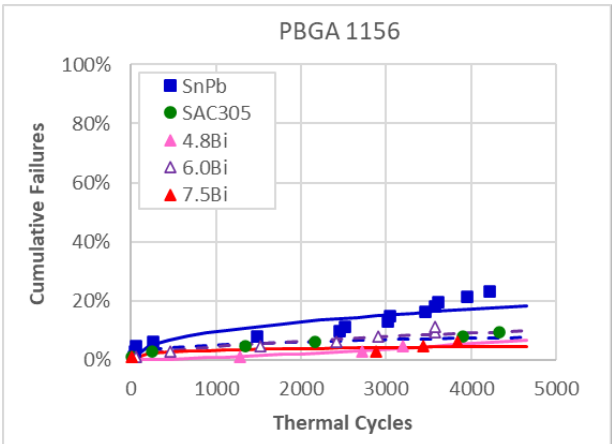

PBGA 1156	β	N63	R^2	Failed	# Samples	Failure Rate
SnPb	0.454	1.59E+05	89%	14	59	23.7%
SAC305	0.277	4.41E+07	95%	6	60	10.0%
4.8Bi	1.395	3.16E+04	97%	3	60	5.0%
6.0Bi	0.517	3.78E+05	95%	7	60	11.7%
7.5Bi	0.227	3.34E+09	83%	4	60	6.7%

Figure 5: PBGA-1156 Statistics by Solder Alloy, All Fails

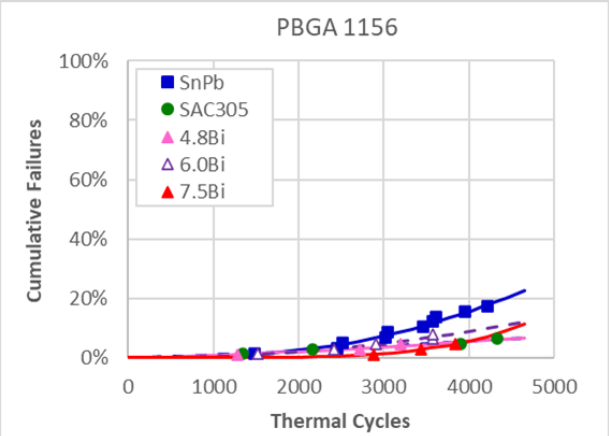

PBGA 1156	β	N63	R^2	Failed	# Samples	Failure Rate
SnPb	2.753	7.63E+03	97%	10	55	18.2%
SAC305	1.325	3.52E+04	96%	4	58	6.9%
4.8Bi	1.395	3.16E+04	97%	3	60	5.0%
6.0Bi	2.142	1.21E+04	98%	5	58	8.6%
7.5Bi	4.787	7.25E+03	100%	3	59	5.1%

Figure 6: PBGA-1156 Statistics by Solder Alloy, Excluding Failures Below 500 Cycles

Physical Failure Analysis

Metallographic cross-sectional analysis was conducted on the PBGA-1156 components to document the solder joint failure location, crack morphology, and solder joint microstructure. General physical failure observations of the failed PBGA-1156 components were:

- Solder joint cracks initiated at the solder joint/component pad interface. The crack formation and location conform to industry knowledge of PBGA failure modes [3, 5].
- The solder joint geometries and wetting angles were acceptable and met industry workmanship criteria. While some were observed in the solder joints, their presence was not detrimental to the solder joint integrity.
- The solder joint microstructures were homogeneous with no segregated regions and the solder ball alloy dominated the microstructure as it provided the largest material contribution to the solder joint formation.

Figure 7 through Figure 11 illustrate the typical PBGA-1156 solder joint failures observed:

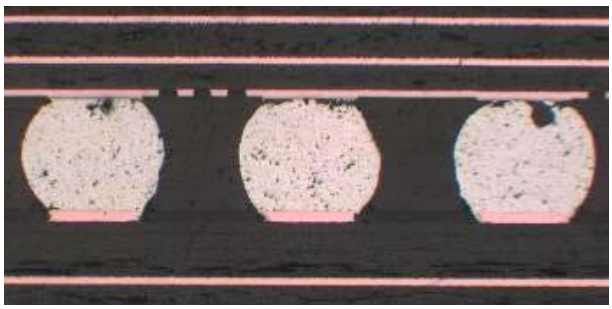

Figure 7: PBGA-1156 SnPb Solder, Failed at 50 Cycles

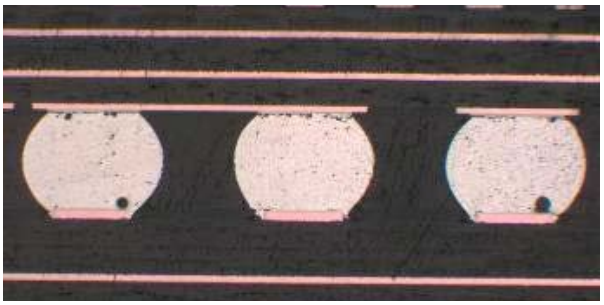

Figure 8: PBGA-1156 SAC305 Solder, Failed at 241 Cycles

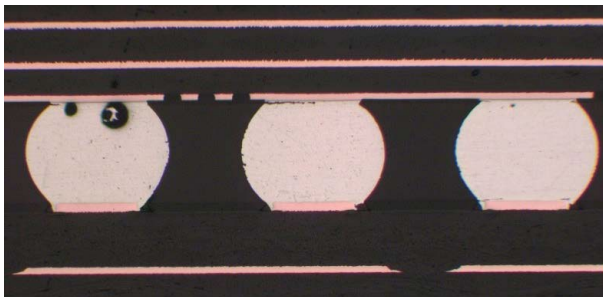

Figure 9: PBGA-1156 SAC4.8Bi Solder, Failed at 2720 Cycles

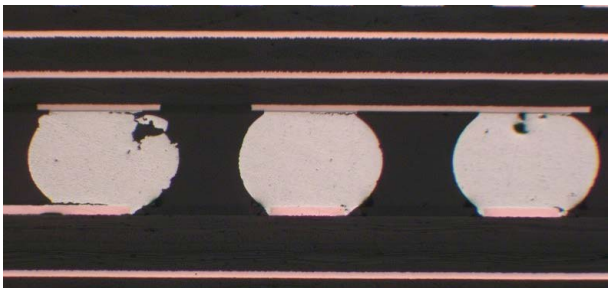

Figure 10: PBGA-1156 SAC6.0Bi Solder, Failed at 56 Cycles

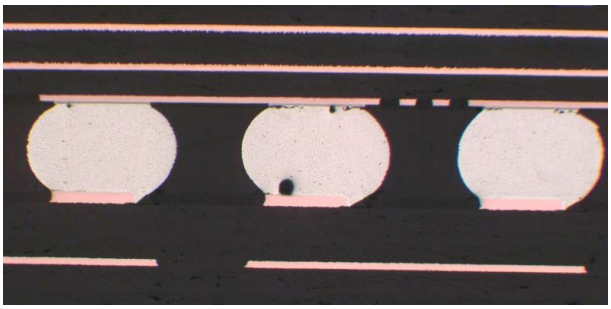

Figure 11: PBGA-1156 SAC7.5Bi Solder, Failed at 3442 Cycles

Plastic Ball Grid Array (PBGA-676) Results

Statistical Analysis

The PBGA-676 components had accumulated 50.6% population failure after the completion of 4362 thermal cycles. SnPb had the highest failure rate at 100% failure, followed by SAC305 at 77.1% failure, while SAC6.0Bi had the lowest failure rate at 16.7%. All of the SACBi alloys performed better than SnPb and SAC305, with most failures occurring after 3000 cycles. Figure 12 and Figure 13 summarize the PBGA-676 thermal cycle test results. Again,

the first plot shows all failure data while the second figure shows filtered data that only includes failures that occurred after 600 thermal cycles to eliminate infant mortality effects from the overall population trends.

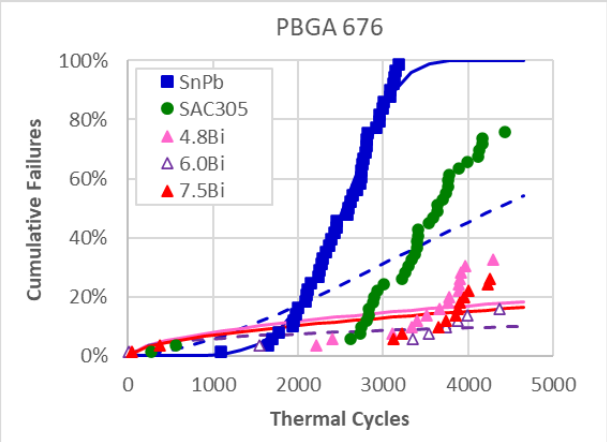

PBGA 676	β	N63	R^2	Failed	# Samples	Failure Rate
SnPb	5.66	2.71E+03	97%	47	47	100.0%
SAC305	1.68	5.39E+03	67%	37	48	77.1%
4.8Bi	0.58	7.28E+04	58%	16	48	33.3%
6.0Bi	0.36	2.43E+06	74%	8	48	16.7%
7.5Bi	0.59	8.62E+04	76%	13	48	27.1%

Figure 12: PBGA-676 Statistics by Solder Alloy, All Fails

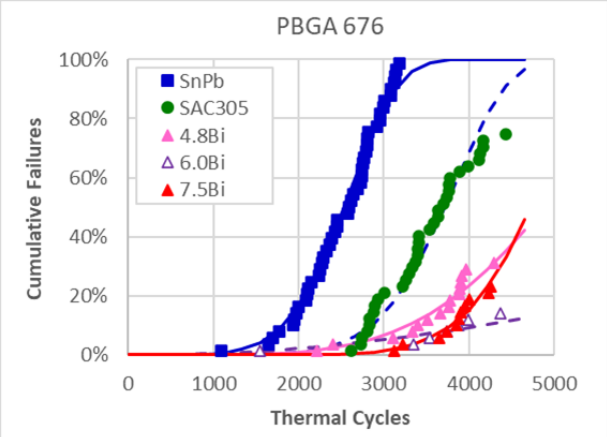

PBGA 676	β	N63	R^2	Failed	# Samples	Failure Rate
SnPb	5.66	2.71E+03	97%	47	47	100.0%
SAC305	7.08	3.92E+03	90%	35	46	76.1%
4.8Bi	4.74	5.29E+03	94%	15	47	31.9%
6.0Bi	2.14	1.19E+04	85%	7	47	14.9%
7.5Bi	8.58	4.93E+03	95%	11	46	23.9%

Figure 13: PBGA-676 Statistics by Solder Alloy, Excluding Failures Below 600 Cycles

Physical Failure Analysis

Metallographic cross-sectional analysis was conducted on the PBGA-676 components to document the solder joint failure location, crack morphology, and solder joint microstructure.

General physical failure observations of the failed PBGA-676 components were:

- The cracks in the solder joints initiated at the solder joint/component pad interface. Some minor cracking was observed at the test vehicle pad/solder joint interface. The crack formation and location are in agreement with industry knowledge of PBGA failure modes [3,5].
- The solder joint geometries and wetting angles were acceptable and met industry workmanship criteria. There were multiple instances of voids observed in the solder joints, but their presence was not detrimental to the solder joint integrity.
- The manufactured test vehicle solder joint microstructures were homogenous with no segregation regions. The solder ball alloy dominated the microstructure as it provided the largest material contribution to the solder joint formation. Some instances of large intermetallic compound (IMC) phases were observed, but they typically had minimal interaction with the crack failure path.

Figure 14 through Figure 18 illustrate the typical PBGA-676 solder joint failures observed:

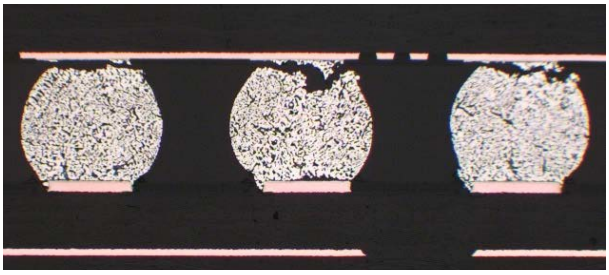

Figure 14: PBGA-676 SnPb Solder, Failed at 1088 Cycles

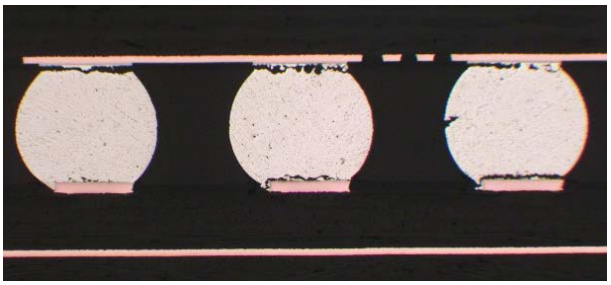

Figure 15: PBGA-676 SAC305 Solder, Failed at 273 Cycles

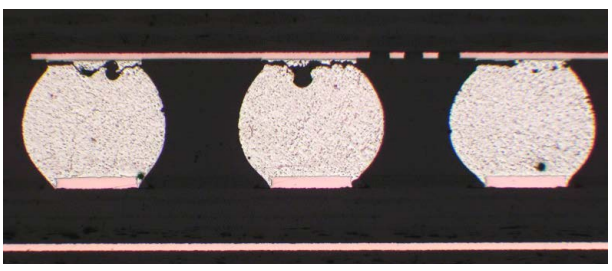

Figure 16: PBGA-676 SAC4.8Bi Solder, Failed at 2209 Cycles

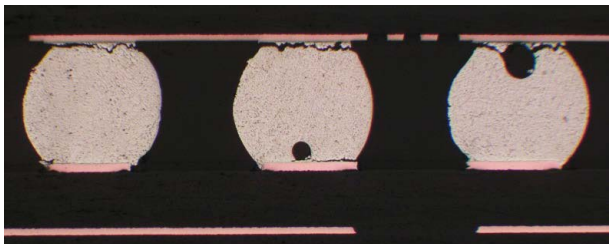

Figure 17: PBGA-676 SAC6.0Bi Solder, Failed at 3871 Cycles

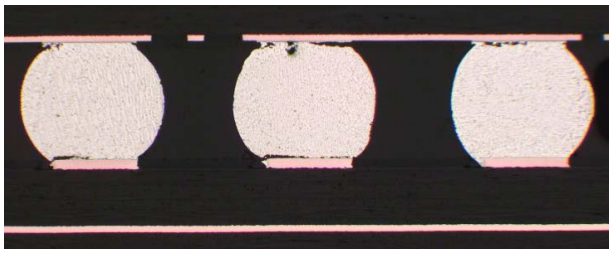

Figure 18: PBGA-676 SAC7.5Bi Solder, Failed at 3166 Cycles

Testing showed that the PBGA-676 component was less reliable than the PBGA-1156 component. Figure 19 illustrates the observed trend for the SnPb solder alloy with the PBGA-676 failing earlier than the PBGA-1156. This plot shows the results for a single combination of laminate and surface finish (408HR with ENIG); other board/surface finish combinations tended to show similar results.

Normally, larger BGA components tend to have lower reliability in thermal cycling than smaller BGA components, as the larger components imposes greater stress/strain on the solder joints resulting in earlier failure. Additional investigation revealed that the PBGA-676 (27mm x 27mm package with a 17mm x 17mm die) had a larger internal die than the PBGA-1156 (37mm x 37mm package with a 15mm x 15mm die). The smaller size of the PBGA-676 coupled with a larger die size exacerbates the coefficient of thermal expansion (CTE) mismatch stresses on solder joints. This was most prominent in the SnPb solder alloy and to a lesser degree for the Pb-free solder alloys in this investigation.

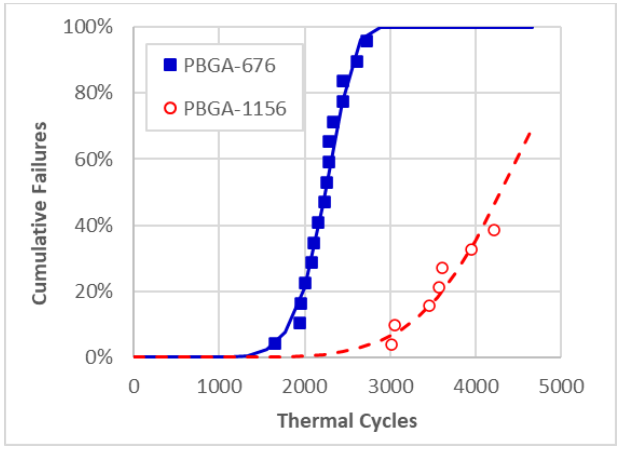

Figure 19: Comparing PBGA-1156 to PBGA-676 reliability (408HR Laminate/ENIG Surf. Fin./SnPb Alloy)

The specific combination of solder alloy, laminate and surface finish did affect reliability, as illustrated in Figure 20. This compares component failure rates for the two PBGAs when testing finished. In each case, more of the smaller PBGAs had failed by the end of testing. In most cases, results were similar for the two laminate materials and in only two out of ten Component/Solder combinations the ENIG surface finish led to higher failure rates.

The impact of board laminate and surface finish on the failure rates of these two BGA packages corresponds to slightly higher stress in the board and reduced compliance in the solder, which exacerbates the increased stress effects induced by the larger die in the smaller package. This will be discussed further in a later section of this document in which the influences of laminate and surface finish on component reliability are discussed.

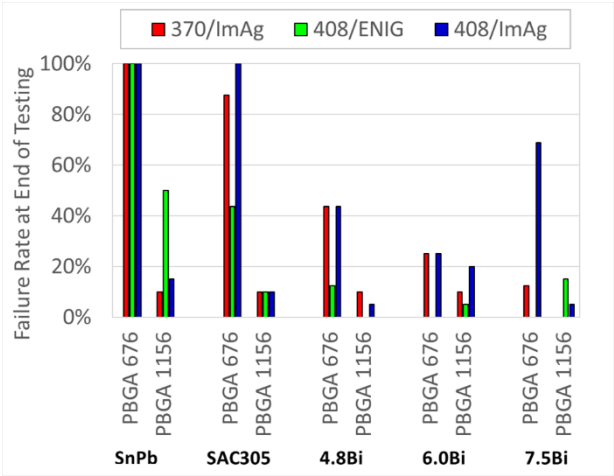

Figure 20: Overall Failure Rate for PBGA Packages with Different Board/Surface Finish/Solder Alloy Combinations

Ceramic Leadless Chip Carriers (CLCC-20) Results
Statistical Analysis

The CLCC-20 components had accumulated an overall 99.2% failure after 4362 thermal cycles. It is important to note that the SnPb and SAC305 data show that there was one component of each alloy that didn't fail, cross- sectional analysis revealed that those components were complete cracked, but still electrically conductive below the failure threshold. The CLCC-20 components were included on the test vehicles because of their poor reliability track record on electronic assemblies used in harsh environments. Industry data [6] has demonstrated that the CLCC component style undergoes solder joint integrity degradation under IPC Class 3 use environments due to coefficient of thermal expansion (CTE) mismatch with the printed circuit board. The N63 values range from 328 to 1101 cycles. SAC6.0Bi had the best thermal cycle performance with SAC4.8Bi following closely behind, although all the SACBi alloys performed better than SnPb and SAC305.

Figure 21 and Figure 22 summarize the thermal cycle test results.

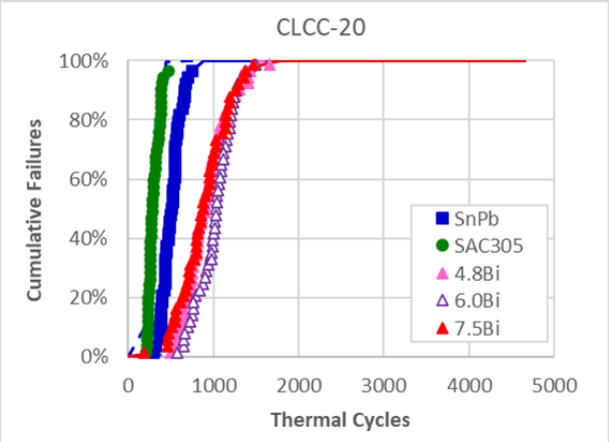

CLCC-20	β	N63	R^2	Failed	# Samples	Failure Rate
SnPb	5.63	5.50E+02	95%	46	47	97.9%
SAC305	5.50	3.28E+02	86%	47	48	97.9%
4.8Bi	4.36	1.01E+03	94%	48	48	100.0%
6.0Bi	5.45	1.10E+03	98%	47	47	100.0%
7.5Bi	3.18	9.90E+02	96%	47	47	100.0%

Figure 21: CLCC Statistics by Solder Alloy, All Fails

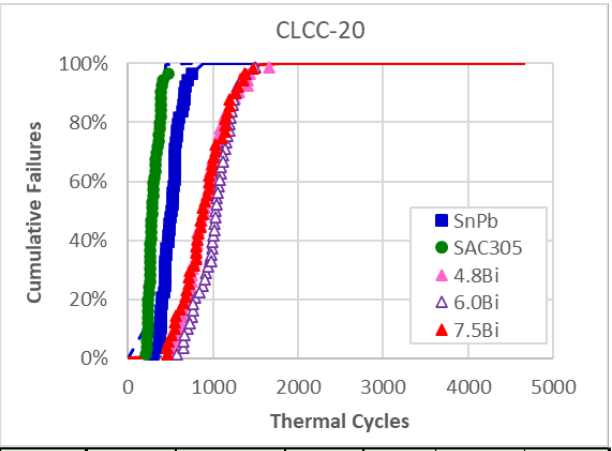

CLCC-20	β	N63	R^2	Failed	# Samples	Failure Rate
SnPb	5.63	5.50E+02	95%	46	47	97.9%
SAC305	5.50	3.28E+02	86%	47	48	97.9%
4.8Bi	4.36	1.01E+03	94%	48	48	100.0%
6.0Bi	5.45	1.10E+03	98%	47	47	100.0%
7.5Bi	3.93	9.88E+02	97%	46	46	100.0%

Figure 22: CLCC-20 Statistics by Solder Alloy, Not Including Failures Below 200 Cycles

Physical Failure Analysis

Metallographic cross-sectional analysis was conducted on the CLCC-20 components to document the solder joint failure location, crack morphology and solder joint microstructure. General physical failure observations of the failed CLCC-20 components were:

- Solder joint cracks initiated under the components and traversed at a ~45° angle through the solder fillets. The crack formation and location agree with industry published data of typical CLCC failure modes [7, 8].
- The solder joint geometries and wetting angles were acceptable and met industry workmanship criteria.

Figure 23 through Figure 27 illustrate the typical CLCC-20 solder joint failures.

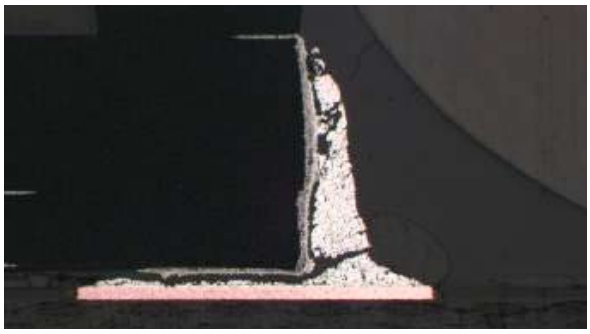

Figure 23: CLCC-20 SnPb Solder, Failed at 328 Cycles

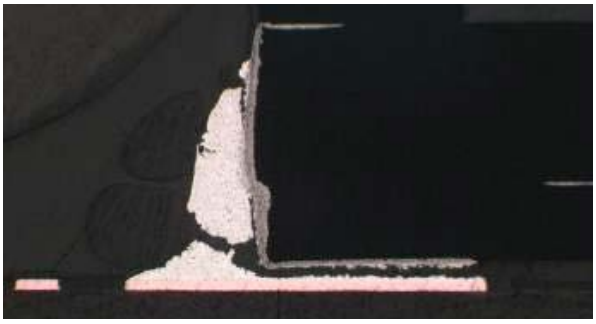

Figure 24: CLCC-20 SAC305 Solder, Failed at 468 Cycles

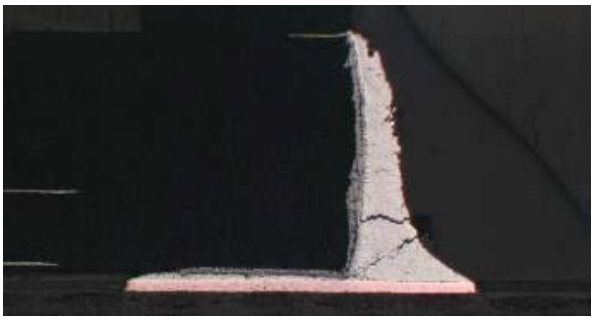

Figure 25: CLCC-20 SAC4.8Bi Solder, Failed at 1041 Cycles

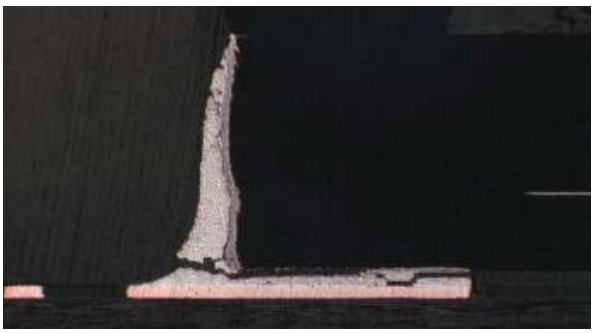

Figure 26: CLCC-20 SAC6.0Bi Solder, Failed at 569 Cycles

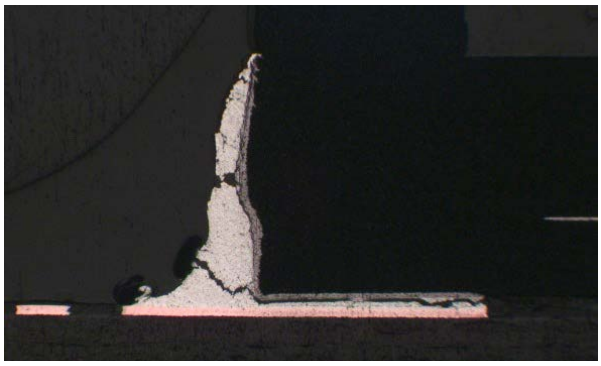

Figure 27: CLCC-20 SAC7.5Bi Solder, Failed at 1468 Cycles

Micro-Lead Frame (MLF-20) Results
Statistical Analysis

The MLF-20 components had accumulated an overall 74.9% population failure after the completion of 4362 thermal cycles. For this component type, SnPb performed significantly better than all of the other alloys, with only 8.3% failure, while all of the SAC alloys amassed over 80% failure. Published results showed that a QFN- 48 package with SnPb solder alloy performed better than a SAC405 solder alloy in 0°C -100°C thermal cycle test conditions [9]. Note that QFN (quad flatpack no-lead) and MLF are different terms for essentially the same package style.

Figure 28 and Figure 29 summarize the MLF-20 thermal cycle test results, again for all data as well as with early (infant mortality) failures removed.

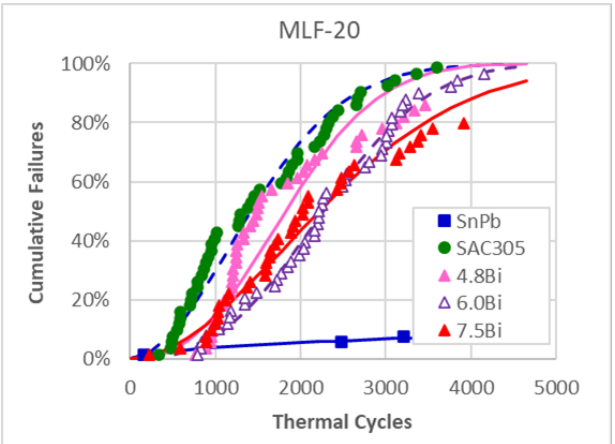

MLF-20	β	N63	R^2	Failed	# Samples	Failure Rate
SnPb	0.54	4.14E+05	99%	4	48	8.3%
SAC305	1.91	1.72E+03	94%	48	48	100.0%
4.8Bi	2.43	2.12E+03	79%	42	48	87.5%
6.0Bi	2.67	2.60E+03	97%	46	47	97.9%
7.5Bi	1.89	2.69E+03	96%	39	48	81.3%

Figure 28: MLF-20 Statistics by Solder Alloy, All Fails

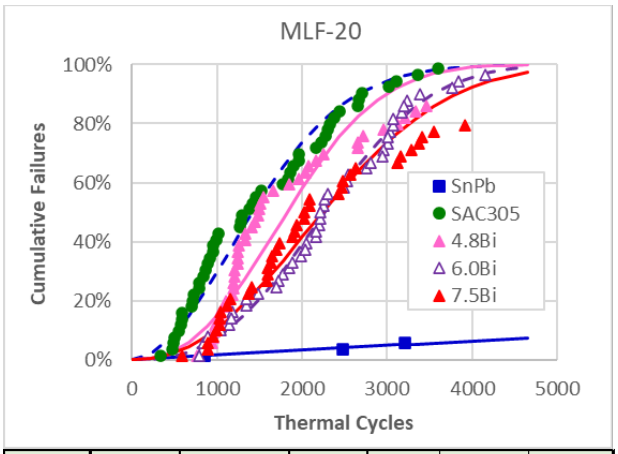

MLF-20	β	N63	R^2	Failed	# Samples	Failure Rate
SnPb	0.98	6.47E+04	97%	3	47	6.4%
SAC305	1.91	1.72E+03	94%	48	48	100.0%
4.8Bi	2.43	2.12E+03	79%	42	48	87.5%
6.0Bi	2.67	2.60E+03	97%	46	47	97.9%
7.5Bi	2.26	2.64E+03	93%	38	47	80.9%

Figure 29: MLF-20 Statistics by Solder Alloy, Not Including Failures Below 250 Cycles

The MLF-20 Weibull statistics reveal a significant difference in the SnPb solder alloy and the Pb-free alloys. A MLF is a type of Bottom Terminated Component (BTC) and BTC thermal cycle testing conducted in 2019 [10] did not demonstrate such a large reliability difference between SnPb and Pb-free alloys. Those tests found much better reliability, with Weibull N63 values for SnPb solder and SAC305 solder of 5421 cycles and 3179 cycles respectively.

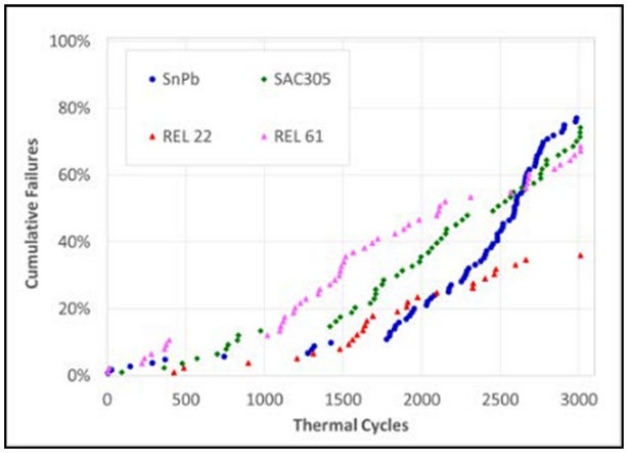

Figure 30: BTC Thermal Cycle Results, Cumulative failures, 10mm MLF72, 0.5mm pitch [10]

A detailed investigation using non-cycled MLF-20 package cross-sections revealed the root cause for the difference. Because the packages were dimensionally identical except for surface finish, the test vehicle design used the same MLF-20 footprint for the SnPb and Pb-free solder alloys. However, the procured Pb-free MLF-20 components had larger footprints than their SnPb counterparts (Figure 31), which led

to solder joint bridging between the central thermal pad and the I/O pads (Figure 32). The solder bridging changed the solder joint geometry and contact area, which affected the thermal cycle reliability. This package size issue confounds the data, which prevents directly comparing reliability results of components with SnPb solder to those with Pb-free solder alloys.

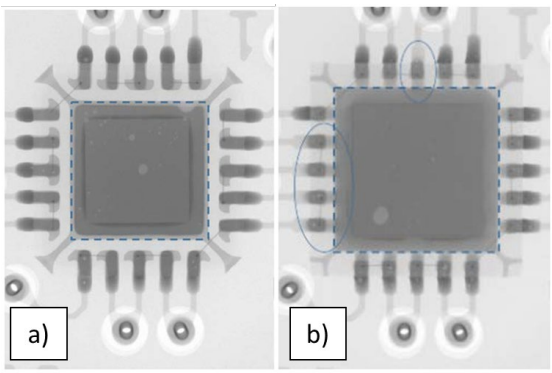

Figure 31: MLF-20 Component Footprint Discrepancy Showing Package Size and Solder Bridging; a) SnPb Solder, b) SAC305 Solder

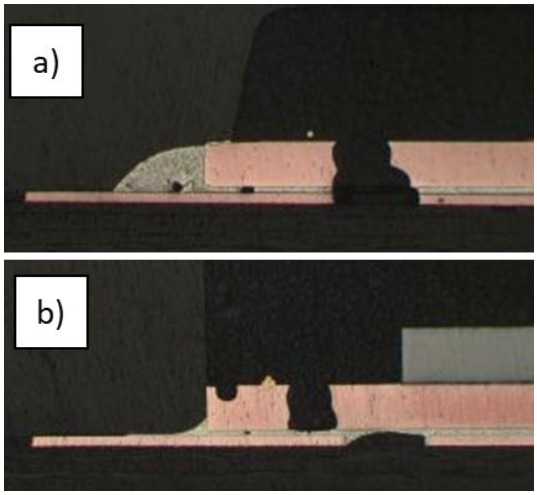

Figure 32: MLF-20 Solder Bridging Due to Component Dimension Issue; a) SnPb Solder, b) SAC305 Solder

Physical Failure Analysis

Metallographic cross-sectional analysis was conducted on the MLF-20 components to document the solder joint failure location, crack morphology, and solder joint microstructure. It should be noted that the MLF-20 components contained a metallized thermal pad that was soldered to the test vehicles that has a significant influence on the thermal cycle solder joint integrity. General physical failure observations of the failed MLF-20 components were:

- The cracks in the I/O solder joints initiated in the bottom terminated pads and traversed towards the lead toe. The crack formation and location agree with industry published data [9, 11].
- The I/O solder joint geometries and wetting angles were acceptable and met industry workmanship criteria. The ground pad on the MLF-20 components achieved 50% minimum solder coverage and no cracking was observed in that solder joint.

Figure 33 through Figure 37 illustrate the typical MLF-20 solder joint failures.

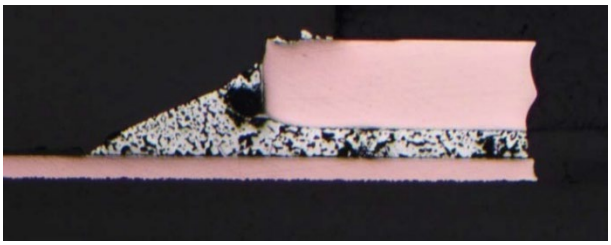

Figure 33: MLF-20 SnPb Solder, Did Not Fail

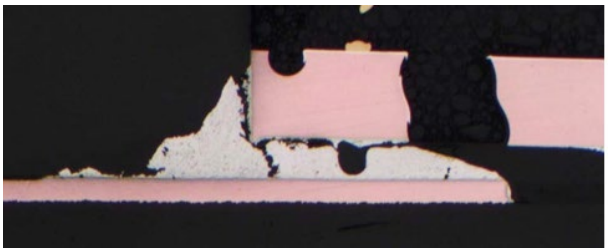

Figure 34: MLF-20 SAC305 Solder, Failed at 332 Cycles

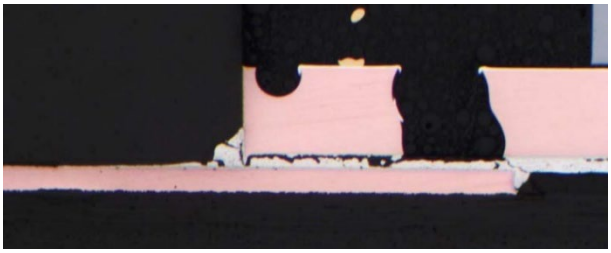

Figure 35: MLF-20 SAC4.8Bi Solder, Failed at 759 Cycles

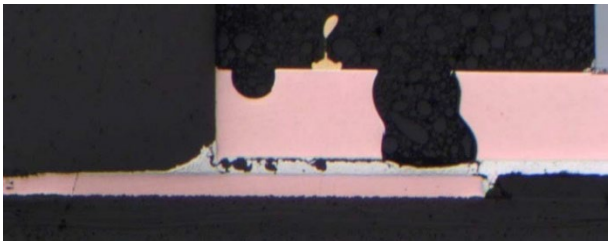

Figure 36: MLF-20 SAC6.0Bi Solder, Failed at 784 Cycles

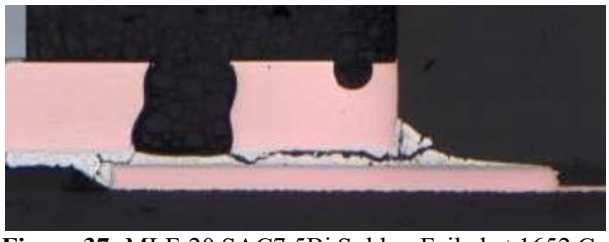

Figure 37: MLF-20 SAC7.5Bi Solder, Failed at 1652 Cycles

Small Outline Transistor (SOT-23) Results

Statistical Analysis

Overall, 42% of the SOT-23 components failed after 4362 thermal cycles. The SACBi alloys performed better than the SnPb and SAC305. The SAC6.0Bi alloy performed significantly better than the others, with no failures until after 3500 cycles and an overall 12.5% failure rate.

Figure 38 and Figure 39 show SOT-23 results, again with separate plots for all data and with early failures filtered out.

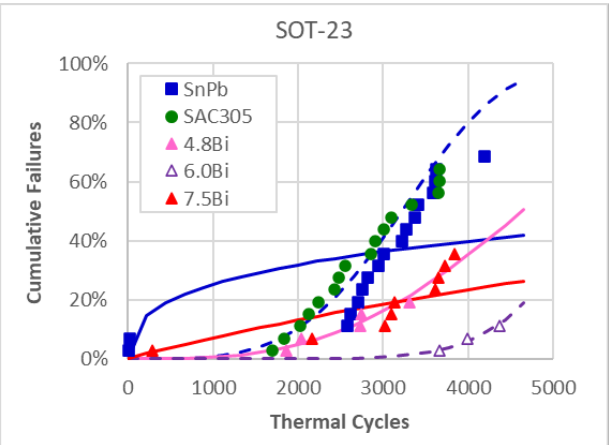

SOT-23	β	N63	R^2	Failed	# Samples	Failure Rate
SnPb	0.41	2.13E+04	65%	17	24	70.8%
SAC305	3.90	3.54E+03	94%	16	24	66.7%
4.8Bi	3.14	5.21E+03	89%	5	24	20.8%
6.0Bi	7.89	5.68E+03	96%	3	24	12.5%
7.5Bi	0.92	1.68E+04	75%	9	24	37.5%

Figure 38: SOT-23 Statistics by Solder Alloy, All Fails

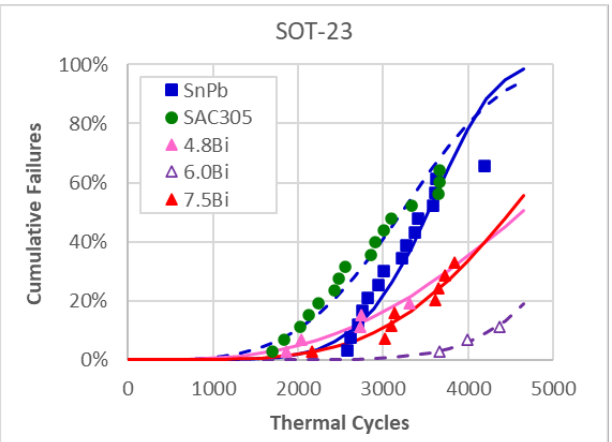

SOT-23	β	N63	R^2	Failed	# Samples	Failure Rate
SnPb	6.44	3.74E+03	84%	15	22	68.2%
SAC305	3.90	3.54E+03	94%	16	24	66.7%
4.8Bi	3.14	5.21E+03	89%	5	24	20.8%
6.0Bi	7.89	5.68E+03	96%	3	24	12.5%
7.5Bi	4.47	4.88E+03	94%	8	23	34.8%

Figure 39: SOT-23 Statistics by Solder Alloy, Excluding Failures below 300 Cycles

Physical Failure Analysis

Metallographic cross-sectional analysis was conducted on the SOT-23 components to document the solder joint failure location, crack morphology, and solder joint microstructure. General physical failure observations of the failed SOT-23 components were:

- The cracks in the solder joints initiated in the heel fillet region and traversed under the foot towards the lead toe. The crack formation and location are in agreement with industry knowledge of Alloy 42 lead material/TSOP failure modes [12].
- The solder joint geometries and wetting angles were acceptable and met industry workmanship criteria (IPC-J-STD-001). There were a number of instances where the solder did flow into the upper lead bend region. In most cases, this condition is acceptable per the IPC-J-STD-001/IPC-A-610 specifications.
- The solder joint microstructures were homogenous and uniform. SnPb solder joint microstructure coarsening was observed due to CTE mismatch between the solder and the Alloy 42 lead of the SOT-23.

Figure 40 through Figure 44 illustrate the typical SOT-23 solder joint failures.

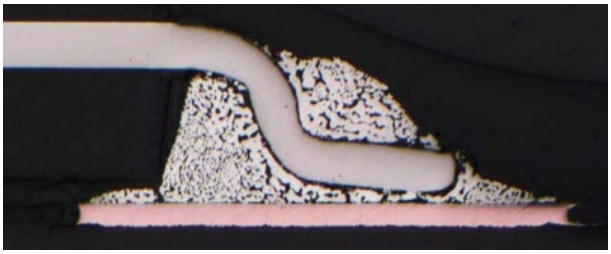

Figure 40: SOT-23 SnPb Solder, Failed at 3004 Cycles

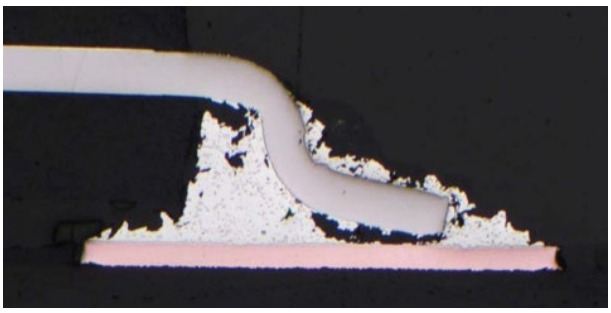

Figure 41: SOT-23 SAC305 Solder, Failed at 2548 Cycles

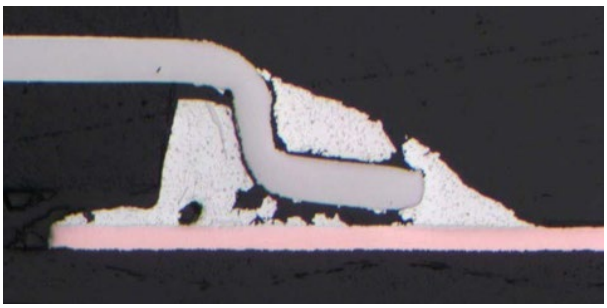

Figure 42: SOT-23 SAC4.8Bi Solder, Failed at 2741 Cycles

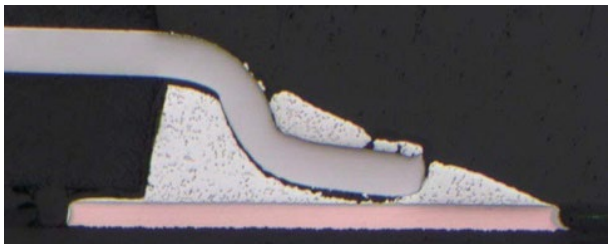

Figure 43: SOT-23 SAC6.0Bi Solder, Failed at 3987 Cycles

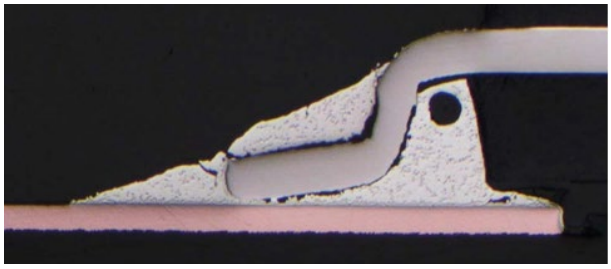

Figure 44: SOT-23 SAC7.5Bi Solder, Failed at 2163 Cycles

Thin Quad Flat Package (TQFP-144) Results

Statistical Analysis

Overall, 85% of the TQFP-144 components had failed after the completion of 4362 thermal cycles. The SAC305 solder performed significantly worse than the other alloys, reaching 100% failure by 2700 cycles. The few early failures of the component were due to manufacturing errors.

Figure 45 and Figure 46 summarize the TQFP-144 thermal cycle test results for full data and with early failures removed.

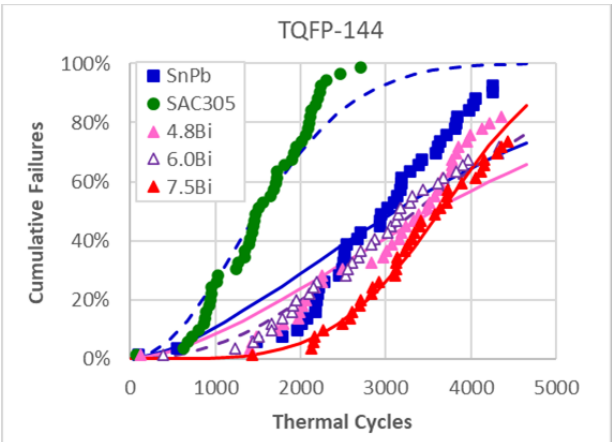

TQFP 144	β	N63	R^2	Failed	# Samples	Failure Rate
SnPb	1.60	3.92E+03	73%	45	48	93.8%
SAC305	1.97	1.82E+03	85%	48	48	100.0%
4.8Bi	1.63	4.45E+03	78%	40	48	83.3%
6.0Bi	2.21	3.96E+03	94%	35	48	72.9%
7.5Bi	4.25	3.97E+03	98%	36	48	75.0%

Figure 45: TQFP-144 Statistics by Solder Alloy, All Fails

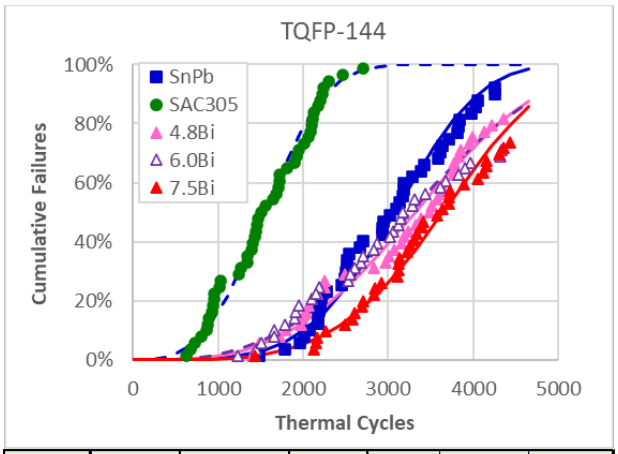

TQFP 144	β	N63	R^2	Failed	# Samples	Failure Rate
SnPb	4.37	3.35E+03	96%	43	46	93.5%
SAC305	3.13	1.74E+03	96%	47	47	100.0%
4.8Bi	3.24	3.71E+03	95%	39	47	83.0%
6.0Bi	3.06	3.68E+03	95%	34	47	72.3%
7.5Bi	4.25	3.97E+03	98%	36	48	75.0%

Figure 46: TQFP-144 Statistics by Solder Alloy, Excluding Failures Below 575 Cycles

Physical Failure Analysis

Metallographic cross-sectional analysis was conducted on the TQFP-144 components to document the solder joint failure location, crack morphology and solder joint microstructure. General physical failure observations of the failed TQFP-144 components were:

- Solder joint cracks initiated in the heel fillet region and traversed under the foot towards the lead toe. The crack formation and location align with industry knowledge of TQFP failure modes [6].
- Solder joint geometries and wetting angles were acceptable and met industry workmanship criteria. In multiple instances, solder did flow into the upper lead bend region, which is acceptable per industry standards.
- The solder joint microstructures were homogenous and uniform. SnPb solder joint microstructure coarsening was observed due to CTE mismatch between the solder and the copper lead base metal of the TQFP-144.

Figure 47 through Figure 51 illustrate the typical TQFP-144 solder joint failures.

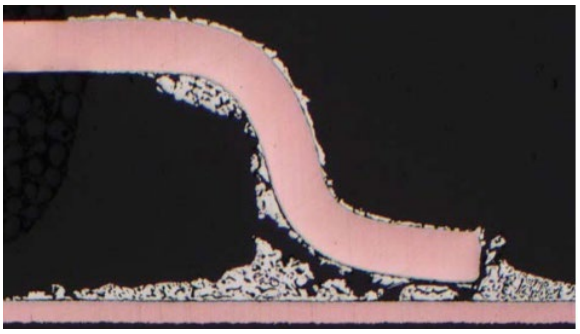

Figure 47: TQFP-144 SnPb Solder, Failed at 2540 Cycles

Figure 48: TQFP-144 SAC305 Solder, Failed at 629 Cycles

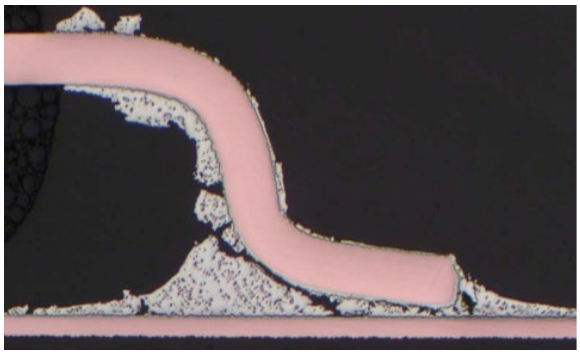

Figure 49: TQFP-144 SAC4.8Bi Solder, Failed at 121 Cycles

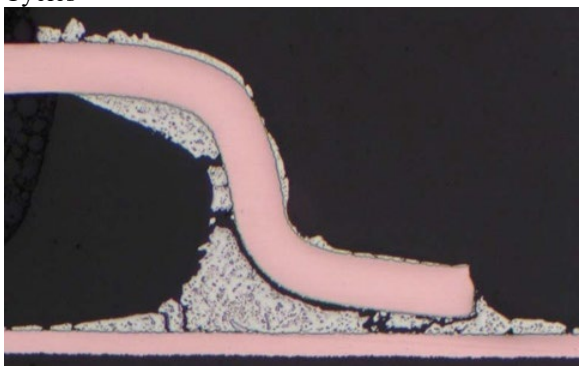

Figure 50: TQFP-144 SAC6.0Bi Solder, Failed at 383 Cycles

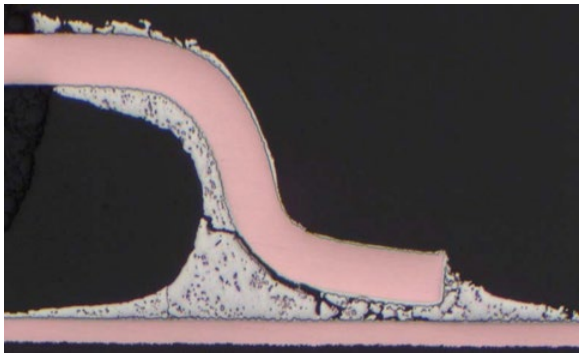

Figure 51: TQFP-144 SAC7.5Bi Solder, Failed at 3123 Cycles

Land Grid Array (LGA) Results

Statistical Analysis

The LGA components had accumulated an overall 13.7% population failure after the completion of 4362 thermal cycles. SnPb had the highest failure rate at 38.3% failure, while SAC4.8Bi and SAC7.5Bi had the lowest at 3.4% and 5% respectively. While all the alloys had low failure rates, the Pb-free alloys performed better than SnPb.

Figure 52 and Figure 53 summarize the LGA thermal cycle test results for the full data set and with early failures removed.

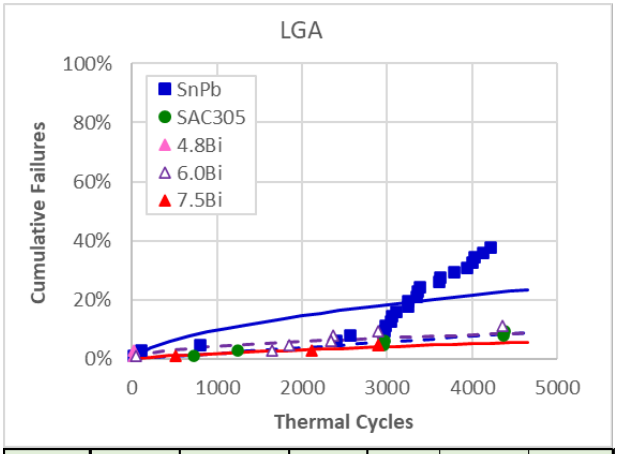

LGA	β	N63	R^2	Failed	# Samples	Failure Rate
SnPb	0.63	3.81E+04	74%	23	60	38.3%
SAC305	1.05	4.44E+04	95%	6	60	10.0%
4.8Bi	n/a	n/a	n/a	2	59	3.4%
6.0Bi	0.48	6.88E+05	81%	7	60	11.7%
7.5Bi	0.74	2.15E+05	97%	3	60	5.0%

Figure 52: LGA Statistics by Solder Alloy, All Fails

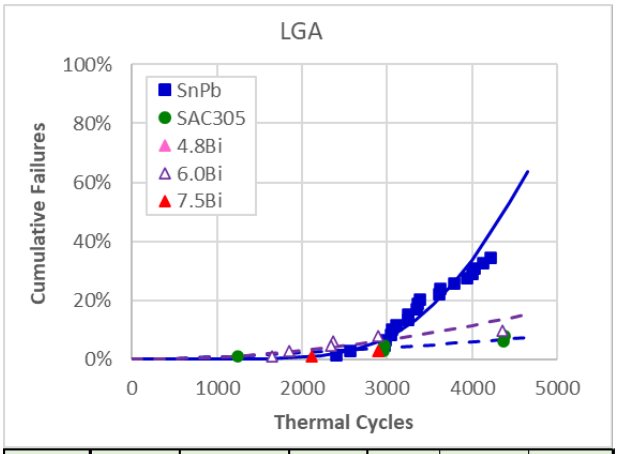

LGA	β	N63	R^2	Failed	# Samples	Failure Rate
SnPb	5.87	4.65E+03	92%	20	57	35.1%
SAC305	1.44	2.81E+04	93%	5	59	8.5%
4.8Bi	n/a	n/a	n/a	0	57	0.0%
6.0Bi	2.01	1.14E+04	78%	6	59	10.2%
7.5Bi	n/a	n/a	n/a	2	59	3.4%

Figure 53: LGA Statistics by Solder Alloy, Not Including Failures Below 900 Cycles

Physical Failure Analysis

Metallographic cross-sectional analysis was conducted on the LGA components to document the solder joint location, crack morphology, and solder joint microstructure. General physical failure observations of the failed LGA components were:

- The cracks in the solder joints initiated at the solder joint/component pad interface.
- The solder joint geometries and wetting angles were acceptable and met industry workmanship criteria. While voids were observed in some solder joints, their presence did not affect the solder joint integrity.
- The test vehicle solder joint microstructures were homogenous with no segregation regions. Solder joint microstructure grain coarsening was evident in the cycled SnPb solder joints. While some examples of large intermetallic compound (IMC) phases were seen, they typically had little interaction with the crack failure path.

Figure 55 though Figure 58 illustrate the typical LGA solder joint failures.

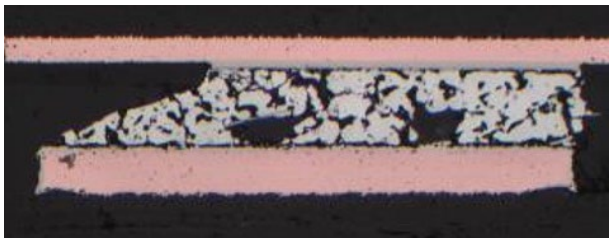

Figure 54: LGA SnPb Solder Alloy – Did Not Fail

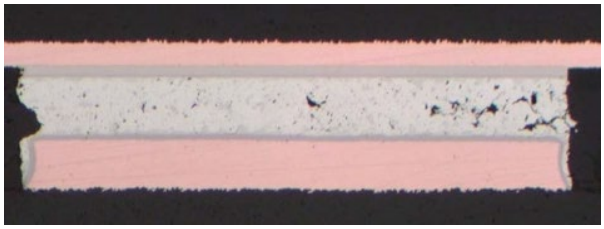

Figure 55: LGA SAC305 Solder Alloy – Did Not Fail

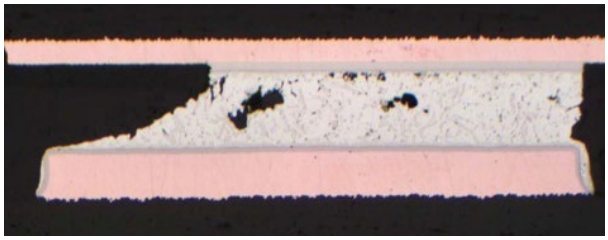

Figure 56: LGA SAC4.8Bi Solder Alloy – Did Not Fail

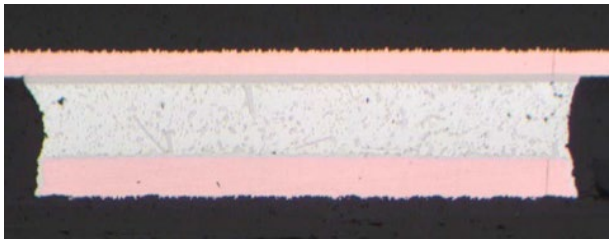

Figure 57: LGA SAC6.0Bi Solder Alloy – Did Not Fail

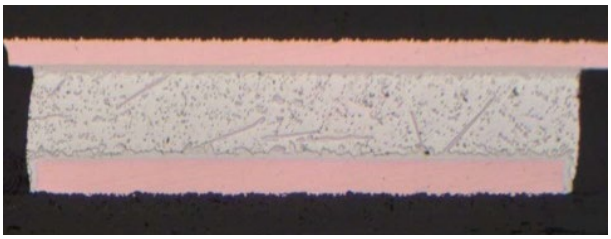

Figure 58: LGA SAC7.5Bi Solder Alloy – Did Not Fail

ENIG vs. ImAg Surface Finish Performance

Members of the IPC/PERM DoD Pb-free Electronics Project team wanted to understand the impact of using either an ImAg or an ENIG board surface finish on solder joint integrity. Industry data [13] show that intermetallic (IMC) formation on copper resulting in the Cu6Sn5 phase is a slightly stronger interface than the IMC formation on nickel resulting in the Ni3Sn4 phase. In most product applications, this IMC phase strength difference has no influence on the overall solder joint integrity. For both surface finishes, the component type plays a larger role in solder joint integrity differences than the board surface finish.

- Figure 59 illustrates this point with the TQFP-144 and PBGA-676 components used in the investigation. There was little difference in SnPb solder joint integrity of TQFP-144 solder joints for the board surface finishes as shown in Figure 59a). However, Figure 59b) illustrates a surface finish bias with the PBGA-676 solder joint on ImAg surface finish performing better than the ENIG surface finish.
- With the SAC305 solder alloy, the board surface finish results are reversed in comparison to SnPb solder alloy. The TQFP-144 component performed better with the ENIG surface finish (Figure 60 a)) and the PBGA-676 component performed better with the ImAg surface finish (Figure 60 b)).
- The SACBi solder alloys had minimal board surface finish bias across the various components in the investigation (Figure 61). The one exception to this trend was the SAC4.8Bi solder alloy, which performed better with the ENIG surface finish (Figure 61 a).

The test data show some measurable impact of the board surface finish impact on solder joint integrity. However, the practical impact of this difference must be considered. As shown in Figure 60 b), the PBGA-676 with ImAg surface finish first failed at ~2500 thermal cycles while components with ENIG surface finish first failed at ~3500 thermal cycles. Since both of these high cycle values are well beyond the 500 or 1000 thermal cycle requirements for use in most avionics systems, the extended life of those parts with ENIG surface finish is really not exploited. A full set of ImAg versus ENIG surface finish graphs can be found in the Appendices.

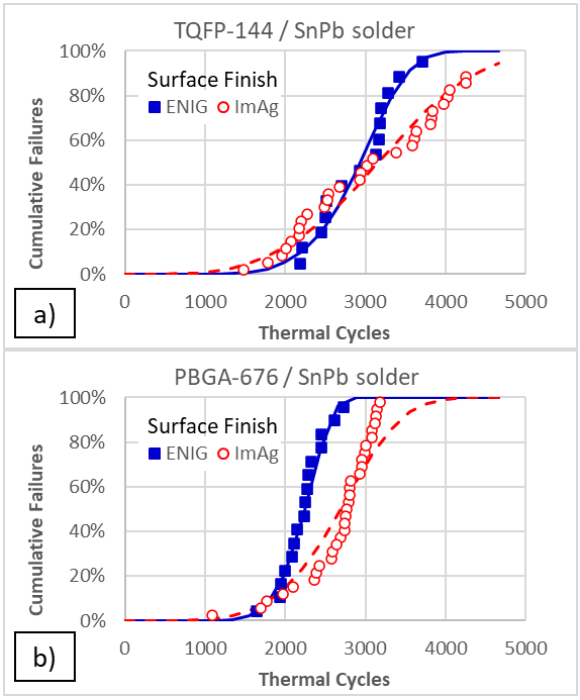

Figure 59: Results for ENIG vs. ImAg for SnPb- Not Including Early Failures; a) TQFP-144, b) PBGA-676

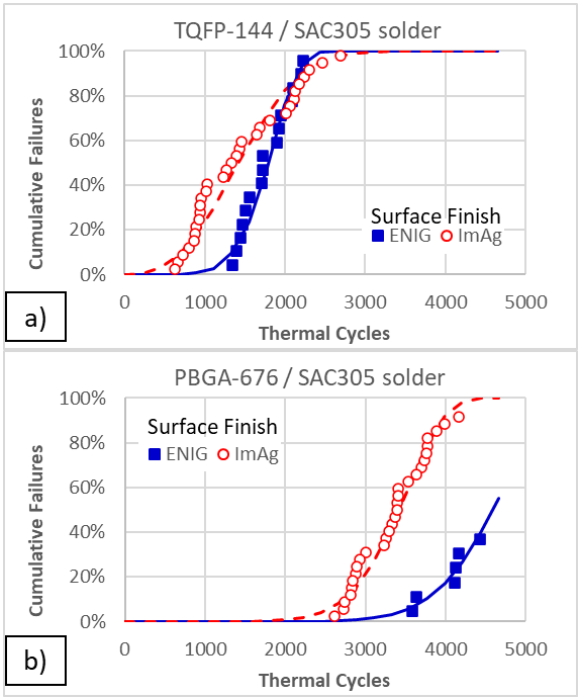

Figure 60: Results for ENIG vs. ImAg for SAC305- Not Including Early Failures; a) TQFP-144, b) PBGA-676

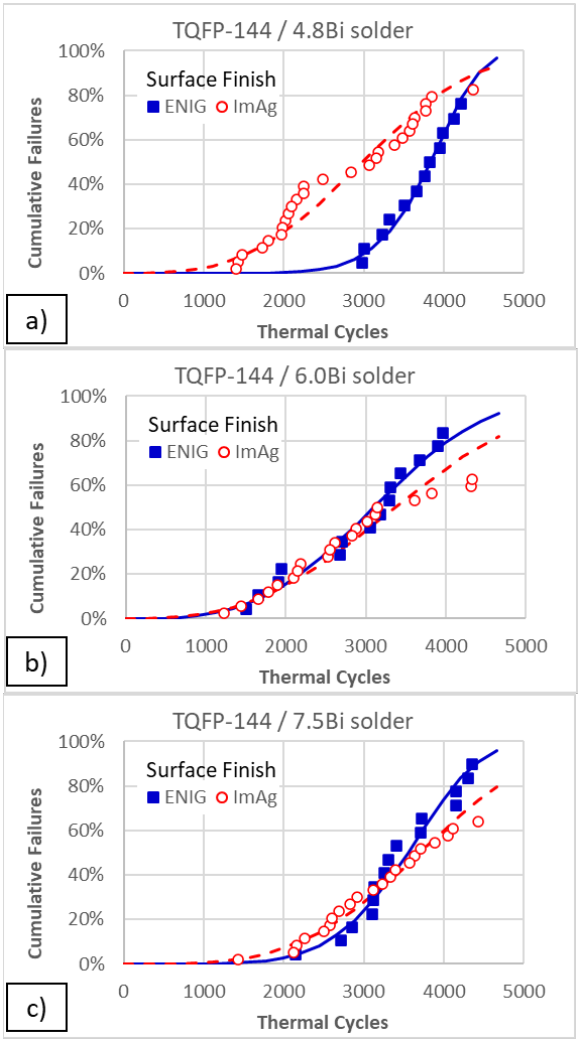

Figure 61: TQFP-144 reliability results for ENIG compared to ImAg - Not Including Early Failures; a) SAC4.8Bi, b) SAC6.0Bi, c) SAC7.5Bi

Isola 408HR vs. Isola 370HR Laminate Performance

The IPC/PERM DoD Phase 3 Pb-free Project investigation included a new variable in the test matrix: the test vehicle laminate type. The previous Joint Council on Aging Aircraft/Joint Group on Pollution Prevention (JCAA/JGPP) Pb-free Solder Project [1] and the NASA DoD Phase 2 Projects [2] used only the Isola 370HR laminate for the test vehicle to keep the test matrix smaller and to allow direct project results comparisons. The inclusion of the Isola 408HR laminate was driven by three primary reasons:

- The NASA-DoD Phase 2 Lead-Free Electronics Project confirmed that pad cratering [2] was one of the dominant failure modes that occur in various board level reliability tests, especially under dynamic loading used to simulate harsh environments.
- Pad cratering is a latent defect that may occur during assembly, rework, and post assembly handling and testing.
- Pad cratering cannot be identified during back-end-of-line in-circuit test (ICT) or functional circuit test (FCT)

protocols and poses a high reliability risk under mechanical and thermo-mechanical loading.

Because the Isola 408HR laminate is more resistant to pad cratering than the Isola 370HR laminate, the investigation team included both materials to assess their influence on the reliability results in the planned vibration and drop shock testing sequences of the IPC/PERM DoD Phase 3 Pb-free Project. Since the laminate type was not expected to significantly affect the solder joint integrity under thermal cycling, one potential combination (Isola 370HR/ENIG surface finish) was not included in the study to increase the available sample sizes for the other combinations .

Figure 62 and Figure 63 show results for the four components that exhibited the most failures by the end of testing (CLCC-20, MLF-20, PBGA-676 and TQFP-144). Each plot compares results for two solder alloys; Figure 62 shows results for SnPb and SAC305 solder while Figure 63 shows results for two of the SAC solder alloys with Bismuth, SAC6.0Bi and SAC7.8Bi. In all these plots, the two prime colors (blue and red) indicate a specific solder alloy. Solid lines/filled symbols show results for components assembled to test boards fabricated with 370HR laminate while dashed lines/open symbols correspond to 408HR. Dark blue and red indicate data for ImAg surface finish and their brighter counterparts (cyan and pink) show results for ENIG surface finish.

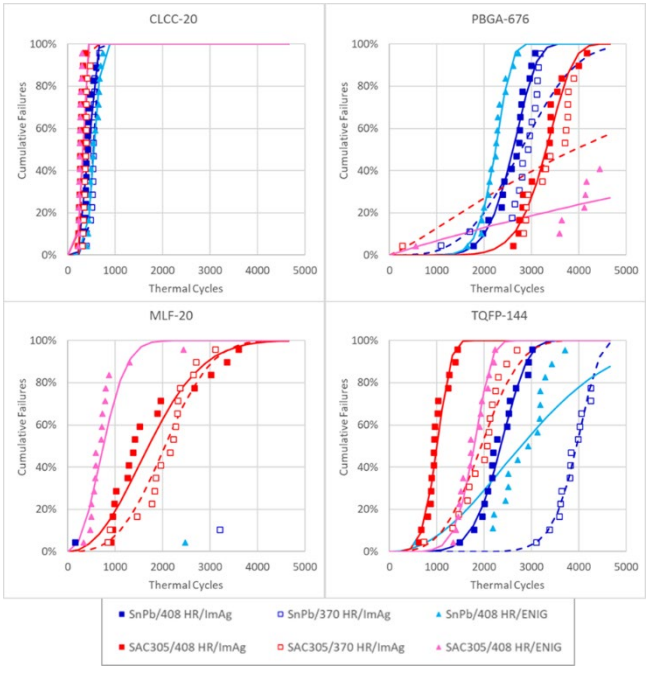

Figure 62: Effect of Laminate/Surface Finish Combination for SnPb and SAC305 Solders

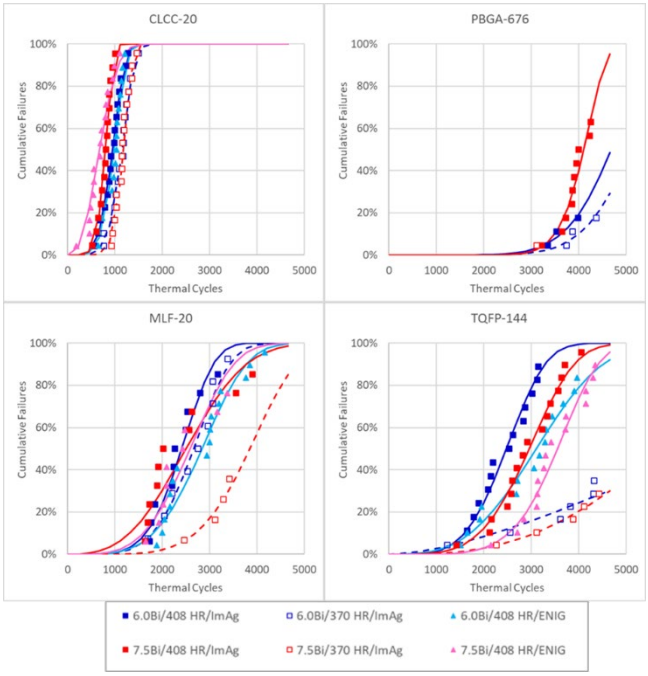

Figure 63: Effect of Laminate/Surface Finish Combination for SAC6.0Bi and SAC7.5Bi Solders

The results demonstrate that there were interaction effects for reliability of a given component / solder / laminate / surface finish combination. The CLCC-20 components exhibited low reliability that was insensitive to the other treatments. The PBGA-676 components with 408HR laminate tended to have higher failure rates with more compliant SnPb and SAC305 solders. However, with the bismuth solder alloys, the components on 370HR boards tended to fail earlier. The MLF-20 components likewise had somewhat lower reliability with the 370HR boards, but only with the SnPb and SAC305 solder alloys. With those solder alloys, the TQFP-144 tended to have lower reliability with the 408 HR laminate, but other components and the bismuth-based solders with that component did not exhibit the same trend.

Discussion

The main "take aways" from the IPC/PERM DoD Pb-free Electronics Project Phase 3 thermal cycle testing project are:

- The PBGA-1156 components performed well for tin-lead (SnPb) with large N63 values (i.e., 2500+ cycles). The lead-free (Pb-free) solder alloys had so few failures that the Weibull statistics could not be calculated.
- The PBGA-676 components performed well for the SnPb and Pb-free solder alloys with high N63 values (i.e., 2000+ cycles) when taking the die size impact into consideration. The SACBi solder alloys performed better than the SnPb and SAC305 solder alloys.
- The CLCC-20 components performed as expected. This component type is known to fail when subjected to extreme temperature cycle ranges and is considered a "high stress" solder joint integrity device. In this investigation, all three SACBi alloys outperformed both SnPb and SAC305.

- The MLF-20 component test data was confounded by the package size/footprint issue making SnPb and Pb-free solder alloy comparison invalid. The SACBi solder alloys performed better than the SAC305 solder alloy. The N63 values were good for all solder alloys (i.e., 1700+ cycles).
- The SOT-23 SACBi components performed well as expected by the investigation team based on industry experience. The solder alloy performance for all solder alloys was good with high N63 values (i.e., 3000+ cycles). The SACBi solder alloys performed better than the SnPb and SAC305 solder alloys.
- The TQFP-144 components performed well for SnPb and Pb-free solder alloys with high N63 values (i.e., 3000+ cycles). The SnPb and SACBi solder alloys performed better than the SAC305 solder alloy.
- The LGA component was a new component style for the consortium as it was not included in the JCAA/JGPP or NASA DoD test programs. All the solder alloys performed well with the Pb-free components having fewer failures than the SnPb components. None of the solder alloys had enough failures to calculate valid Weibull statistics.
- The solder joint thermal cycle testing results illustrated statistical differences for various component technologies for ImAg and ENIG board surface finishes. However, there is no practical impact of those differences in solder joint integrity of components with ImAg and ENIG surface finishes.
- The solder joint thermal cycle testing results demonstrated no practical impact of the board laminate selection on solder joint integrity

Project Phase Comparison

The continuity of using the same test vehicle design and components in a follow-on test provides a unique opportunity to compare thermal cycle test results over time. Table 3 compares the IPC/PERM DoD Pb-free Electronics Project Phase 3/Part 1 study, the Joint Council on Aging Aircraft/Joint Group on Pollution Prevention (JCAA/JGPP) Pb-free Solder Project [1] and NASA DoD Phase 2 Pb-free Solder Project [2] results for the TQFP-144 component. Nearly 16 years span the different test results but overall, there is consistency in the Weibull N63 value for both SnPb solder and for the Pb-free solder alloys. Small changes in the component material composition and the assembly processes account for small differences in thermal cycles for the SnPb solder alloys. For the Pb-free solder alloys, the primary difference is the change in solder alloy composition across the different program phases.

Table 3: TQFP-114, SnPb Solder Thermal Cycle Results

Characteristic Life (N63)			
Solder	***JCAA/JGPP***	***NASA DoD***	***IPC/PERM DoD***
SnPb	2681	3003	3351
SAC305		1774	1740
SAC396	3626		
SAC3.3Bi	3988		
SAC4.8Bi			3714

Acknowledgements

The authors would like to thank IPC/PERM and Collins Aerospace for project funding, Ken Blazek, Jeff Chumbley, and Matt Dolde for thermal cycle testing and cross section support.

References

1. NASA Technology Evaluation for Environmental Risk Mitigation (TEERM) Principal Center website; http://teerm.nasa.gov
2. NASA-DoD Pb-free Electronics Project Consortium, "NASA-DoD Pb-free Electronics Project Plan"; March 2010
3. R. Coyle et al, “The Effect of Bismuth, Antimony, or Indium on the Thermal Fatigue of High Reliability Pb-Free Solder Alloys”, SMTAI Conference Proceedings, 2018.
4. P. Snugovsky et al, "Microstructure, Defects and Reliability of Mixed Pb-free/SnPb Assemblies", TMS Proceedings, Vi: Materials Processing and Properties, pp. 631-642, 2008.
5. R. Kinyanjui et al, "Solder Joint Reliability of Pb-free Sn-Ag-Cu Ball Grid Array (BGA) Components in Sn-Pb Assembly Process", APEX Proceedings, 2008.
6. J. Lau and Y. Pao, Solder Joint Reliability of BGA, CSP, Flip Chip, and Fine Pitch SMT Assemblies, McGraw Hill, ISBN 0-07- 036648-9.
7. R. Wild, "Some Factors Affecting Leadless Chip Carrier Solder Joint Fatigue Life II", Circuit World, Volume 14, No. 4, pp. 29- 41, 1988.
8. R. Pearson and M. Burke, "Solder Alloy Development for Electronic Chip Carriers", Final Report for Period September 1984- January 1988, AFWAL-TR-88-4215.
9. R. Coyle et al, "Temperature cycling Performance of a Quad Flat No Lead (QFN) Package Assembled with Multiple Pb-free Solders", SMTAI Conference Proceedings, Paper AAT 1.2, October 2011.
10. T. Pearson et al, “Solder Joint Integrity Evaluation of Bottom Terminated Component (BTC) Subjected to Thermal Cycling”, SMTAI Conference Proceedings, Chicago, 2019.
11. J. Songnaniuck et al, "Quad Flat No Lead (QFN) Package Processing in High Thermal Mass Assembly", SMTAI Conference Proceedings, Paper AAT4.1, October 2010.
12. P. Viswanadham and P. Singh, Failure Modes and Mechanisms in Electronic Packages, Chapman & Hall, ISBN 0-412-10591-8.
13. P. Tegehall, Review of the Impact of Intermetallic Layers on the Brittleness of Tin-Lead and Lead-free Solder Joints, IVF Project Report 06/07, March 2006.

Appendix A - N1/N10/N63 Solder Performance for -55°C to +125°C Thermal Cycle Testing

Component	*Solder Alloy*	*1st Failure*		*N10*		*N63*	
PBGA-1156	SnPb	27 (1485)		1128 (3367)		1.59e5 (7626)	
	SAC305	3 (1345)	-	12951 (6442)	++	4.4e7 (35266)	++
	SAC4.8Bi	1278	-	6300	++	31625	++
	SAC6.0Bi	56 (1523)	0	4855 (4244)	++	378219 (12133)	++
	SAC7.5Bi	9 (2878)	++	1.62e5 (4532)	++	334e8 (7253)	0
PBGA-676	SnPb	1088		1820		2710	
	SAC305	273 (2645)	++	1416 (2850)	++	5392 (3916)	++
	SAC4.8Bi	29 (2209)	++	1504 (3289)	++	72768 (5287)	++
	SAC6.0Bi	13 (1543)	++	4665 (4162)	++	2.42e6 (11931)	++
	SAC7.5Bi	51 (3116)	++	1915 (3792)	++	86164 (4928)	++
CLCC-20	SnPb	300		369		550	
	SAC305	213	--	218	--	328	--
	SAC4.8Bi	494	++	606	++	1014	++
	SAC6.0Bi	569	++	729	++	1101	++
	SAC7.5Bi	184 (460)	++	487 (558)	++	990 (989)	++
MLF-20	SnPb	160 (850)		6361 (6462)		4.13e5 (64698)	
	SAC305	332	--	530	--	1721	--
	SAC4.8Bi	759	-	842	--	2121	--
	SAC6.0Bi	784	-	1118	--	2596	--
	SAC7.5Bi	226 (585)	--	820 (972)	--	2691 (2637)	--
SOT-23	SnPb	3 (2582)		82 (2637)		21251 (3740)	
	SAC305	1693	--	1986	--	3538	-
	SAC4.8Bi	1855	--	2544	0	5212	++
	SAC6.0Bi	3664	++	4268	++	5675	++
	SAC7.5Bi	285 (2163)	-	1462 (2949)	+	16757 (4882)	++
TQFP-144	SnPb	90 (1485)		958 (2003)		3916 (3351)	
	SAC305	76 (629)	--	580 (848)	--	1818 (1740)	--
	SAC4.8Bi	121 (1405)	-	1123 (1856)	-	4451 (3714)	+
	SAC6.0Bi	383 (1231)	-	1432 (1765)	-	3957 (3680)	+
	SAC7.5Bi	1431	0	2339	+	3974	+
LGA	SnPb	18 (2399)		1059 (3167)		38082 (4647)	
	SAC305	720 (1238)	--	5230 (5859)	++	44372 (28102)	++
	SAC4.8Bi	n/a	n/a	n/a	n/a	n/a	n/a
	SAC6.0Bi	48 (1652)	--	6307 (3720)	+	6.88e5 (11375)	++
	SAC7.5Bi	511 (2112)	-	n/a	n/a	n/a	n/a

Notes on Number formats:

- 1st Failure = earliest failure for a component
- N10 = cycles for 10% failure rate per Weibull fit
- N63 = cycles for 63% failure rate pwer Weibull fit
- a = Insufficient failures to generate Weibull parameters
- (xxxx) = Results when failures not considered representative of the population were excluded

Relative comparison to components with SnPb solder

0	same as control or <5% difference
+	+ = 5 to 20%
++	= >20% difference
-	= -5 to -20% difference
--	>=-20% difference
n/a	Insufficient failures

Appendix B – Component Failure Data for -55°C to +125°C Thermal Cycle Testing

Finish	Solder		Failure Data		Failure Data
ENIG	SnPb	TQFP-144	90,554,2186,2209,2447,2504,2513,2703,2932,3129, 3174, 3183, 3190, 3286, 3426, 3713	SOT-23	2621, 2706, 2761, 2821, 3278, 3378, 3608, 3629
	SAC305		1347, 1401, 1450, 1469, 1510, 1561, 1712, 1720, 1722, 1903, 1927, 1947, 2083, 2106, 2203, 2231		1835, 2019, 2239, 2479, 2852, 3647, 3664 + 1x DNF
	SAC4.8Bi		121, 2975, 3002, 3234, 3327, 3514, 3665, 3758, 3831, 3949, 3989, 4128, 4221 + 3x DNF		8x DNF
	SAC6.0Bi		1508, 1653, 1912, 1948, 2681, 2708, 3059, 3177, 3290, 3309, 3436, 3673, 3904, 3961+ 2x DNF		3987, 4368 + 6x DNF
	SAC7.5Bi		2151, 2711, 2850, 3113, 3123, 3137, 3264, 3304, 3415, 3715, 3730, 4151, 4153, 4307, 4353 + 1x DNF		2163, 3646 + 6x DNF
ImAg	SnPb		1485, 1788, 1957, 2007, 2079, 2170, 2171, 2199, 2275, 2485, 2521, 2540, 2673, 2929, 2940, 3022, 3099, 3380, 3591, 3613, 3636, 3811, 3821, 3840, 3982, 4025, 4057, 4252, 4255 + 3x DNF		3, 21, 2582, 2940, 3004, 3222, 3407, 3591, 4188 + 7x DNF
	SAC305		76, 629, 671, 728, 806, 870, 880, 892, 934, 941, 948, 957, 1015, 1032, 1237, 1264, 1339, 1397, 1438, 1463, 1652, 1680, 1808, 2013, 2065, 2108, 2129, 2176, 2238, 2303, 2471, 2700		1693, 2123, 2432, 2548, 2901, 3011, 3092, 3339, 3668 + 7x DNF
	SAC4.8Bi		1405, 1432, 1487, 1727, 1803, 1973, 1983, 2025, 2064, 2097, 2159, 2252, 2255, 2495, 2837, 3074, 3163, 3183, 3380, 3483, 3578, 3617, 3633, 3775, 3777, 3847, 4362 + 5x DNF		1855, 2038, 2735, 2741, 3306 + 11x DNF
	SAC6.0Bi		383, 1231, 1449, 1654, 1787, 1898, 2095, 2149, 2190, 2528, 2555, 2610, 2831, 2875, 3022, 3123, 3149, 3613, 3828, 4317, 4326 + 11x DNF		3664 + 15x DNF
	SAC7.5Bi		1431, 2126, 2159, 2262, 2496, 2581, 2605, 2692, 2828, 2919, 3117, 3228, 3339, 3400, 3571, 3642, 3708, 3888, 4057, 4113, 4432 + 11x DNF		285, 3020, 3096, 3139, 3613, 3722, 3842 + 9x DNF
ENIG	SnPb	PBGA-676	1651, 1939, 1952, 2002, 2085, 2111, 2152, 2238, 2254, 2281, 2284, 2329, 2448, 2451, 2613, 2725	PBGA-1156	1, 62, 254, 3021, 3050, 3459, 3572, 3607, 3948, 4220 + 10x DNF
	SAC305		558, 3587, 3642, 4111, 4134, 4167, 4436 + 9x DNF		3, 2159 + 18x DFN
	SAC4.8Bi		29, 3768 + 14x DNF		20x DNF
	SAC6.0Bi		16x DNF		3579 + 19x DNF
	SAC7.5Bi		16x DNF		9, 2878, 3835 + 17x DNF
ImAg	SnPb		1, 1088, 1699, 1777, 1978, 2095, 2369, 2391, 2424, 2578, 2586, 2646, 2690, 2737, 2744, 2759, 2770, 2788, 2800, 2809, 2816, 2925, 2960, 2960, 2994, 3006, 3083, 3085, 3116, 3130, 3144, 3184		27, 50, 1485, 2457, 2518 + 35x DNF
	SAC305		273, 2614, 2727, 2739, 2811, 2829, 2837, 2879, 2896, 2928, 3010, 3228, 3262, 3297, 3331, 3377, 3397, 3401, 3408, 3410, 3540, 3633, 3703, 3734, 3767, 3770, 3777, 3893, 3994, 4169 + 2x DNF		241, 1345, 3897, 4327 + 35x DNF
	SAC4.8Bi		2209, 2397, 3111, 3331, 3394, 3512, 3662, 3775, 3886, 3889, 3897, 3920, 3969, 4291 + 18x DNF		1278, 2720, 3200 + 37x DNF
	SAC6.0Bi		13, 1543, 3346, 3534, 3739, 3871, 3992, 4368 + 24x DNF		56, 456, 1523, 2415, 2913, 3574 + 34x DNF
	SAC7.5Bi		51, 370, 3116, 3223, 3645, 3737, 3855, 3875, 3901, 3954, 4003, 4230, 4254 + 19x DNF		3442 + 39x DNF
ENIG	SnPb	CLCC-20	403, 427, 442, 444, 454, 471, 481, 526, 530, 574, 638, 645, 664, 669, 697, 746	LGA	18, 2399, 2570, 2974, 2983, 3048, 3055, 3107, 3248, 3251, 3345, 3358, 3391, 3614, 3620, 3791, 4008, 4032, 4127, 4214
	SAC305		218, 223, 224, 233, 237, 240, 250, 254, 256, 257, 260, 266, 276, 283, 297, 297		2960, 2967 + 18x DNF
	SAC4.8Bi		494, 568, 696, 749, 752, 799, 812, 870, 968, 979, 1068, 1236, 1301, 1413, 1436, 1665		1, 25 + 18x DNF
	SAC6.0Bi		1, 653, 662, 726, 756, 944, 972, 1010, 1033, 1033, 1047, 1074, 1117, 1142, 1161, 1208		48, 1851, 2338, 2364 + 16x DNF
	SAC7.5Bi		184, 460, 462, 479, 546, 551, 558, 681, 691, 712, 799, 816, 848, 948, 981, 1102		511, 2112, 2890 + 17x DNF
ImAg	SnPb		1, 300, 328, 374, 379, 383, 389, 390, 392, 395, 431, 432, 435, 437, 475, 482, 505, 518, 526, 532, 544, 545, 547, 550, 551, 553, 562, 570, 583, 606, 671 + 1x DNF		106, 807, 3937 + 36x DNF
	SAC305		213, 234, 238, 238, 252, 260, 264, 267, 271, 275, 282, 290, 302, 309, 323, 324, 325, 333, 350, 358, 361, 367, 369, 382, 386, 386, 387, 389, 393, 413, 468 + 1x DNF		720, 1238, 4364, 4377+ 35x DNF
	SAC4.8Bi		565, 611, 630, 646, 646, 647, 711, 712, 743, 770, 772, 806, 813, 813, 846, 897, 906, 910, 933, 943, 959, 970, 986, 1041, 1041, 1071, 1074, 1129, 1131, 1163, 1255, 1403		20 + 37 DNF
	SAC6.0Bi		569,647,699,763,763,789,845,877,901,914,974,985,996,1002,1016,1036,1055,1071, 1088, 1091, 1120, 1172, 1187, 1188, 1220, 1234, 1237, 1271, 1287, 1326, 1385, 1499		1652, 2900, 4353 + 36x DNF
	SAC7.5Bi		1, 517, 614, 646, 711, 728, 778, 798, 808, 831, 846, 882, 882, 904, 926, 951, 956, 993, 1009, 1028, 1032, 1138, 1146, 1147, 1163, 1194, 1197, 1253, 1291, 1354, 1363, 1468		39x DNF
ENIG	SnPb	MLF-20	2479 + 15x DNF		
	SAC305		332, 475, 492, 496, 553, 579, 587, 592, 706, 712, 727, 791, 794, 865, 1298, 2445		
	SAC4.8Bi		958, 1026, 1089, 1105, 1844, 2033, 2251, 2653, 3204, 3340, 3459 + 5x DNF		
	SAC6.0Bi		1882, 1992, 2047, 2159, 2160, 2215, 2307, 2946, 3004, 3005, 3028, 3192, 3232, 3762, 3843, 4159		
	SAC7.5Bi		995, 1028, 1154, 1375, 1588, 1652, 1932, 2024, 2089, 2090, 2425, 2476, 3161, 3367 + 2x DNF		
ImAg	SnPb		160, 850, 3203 + 29x DNF		
	SAC305		840, 892, 918, 950, 953, 985, 1018, 1264, 1283, 1385, 1421, 1459, 1516, 1775, 1830, 1859, 1897, 1964, 1965, 2164, 2229, 2281, 2307, 2322, 2374, 2655, 2672, 2702, 3023, 3111, 3361, 3598		
	SAC4.8Bi		759, 893, 939, 964, 974, 1033, 1178, 1188, 1192, 1206, 1208, 1241, 1245, 1249, 1252, 1326, 1329, 1405, 1441, 1486, 1494, 1503, 1544, 1664, 1958, 2073, 2157, 2650, 2719, 2959, 3118 + 1x DNF		
	SAC6.0Bi		0, 784, 821, 842, 896, 1043, 1139, 1166, 1183, 1339, 1350, 1484, 1691, 1728, 1769, 1843, 2041, 2203, 2212, 2246, 2270, 2497, 2534, 2535, 2758, 2800, 2958, 3069, 3074, 3176, 3384 + 1x DNF		
	SAC7.5Bi		226, 585, 887, 890, 947, 1023, 1047, 1114, 1404, 1593, 1599, 1637, 1696, 1730, 1889, 1916, 2019, 2461, 2566, 2624, 3117, 3285, 3415, 3553, 3912 + 7x DNF		

Appendix D – Failure Graphs by Part, Alloy, and Finish

PBGA-1156

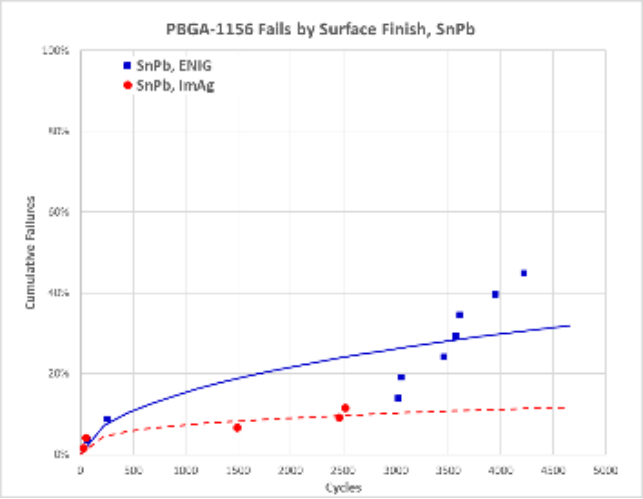

App Figure 1: PBGA-1156 SnPb ENIG vs. ImAg, All Fails

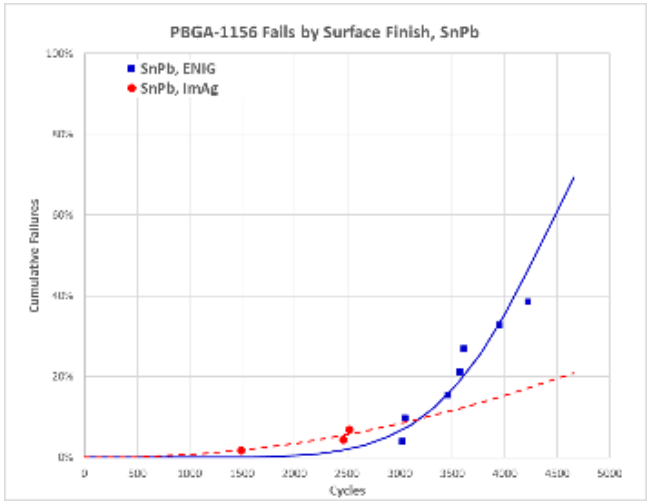

App Figure 2: PBGA-1156 SnPb ENIG vs. ImAg, No Outliers

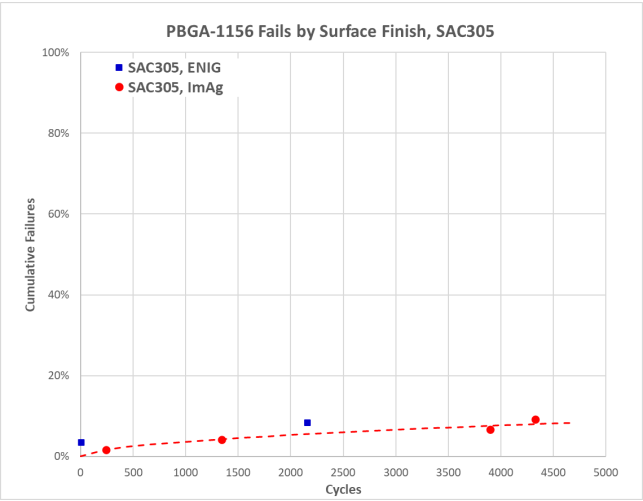

App Figure 3: PBGA-1156 SAC305 ENIG vs. ImAg, All Fails

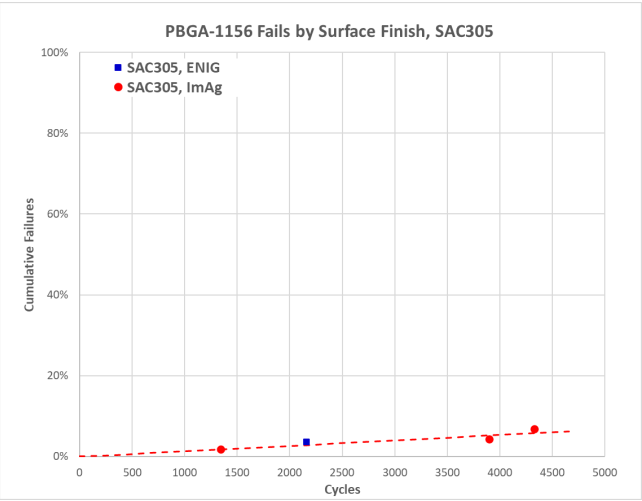

App Figure 4: PBGA-1156 SAC305 ENIG vs. ImAg, No Outliers

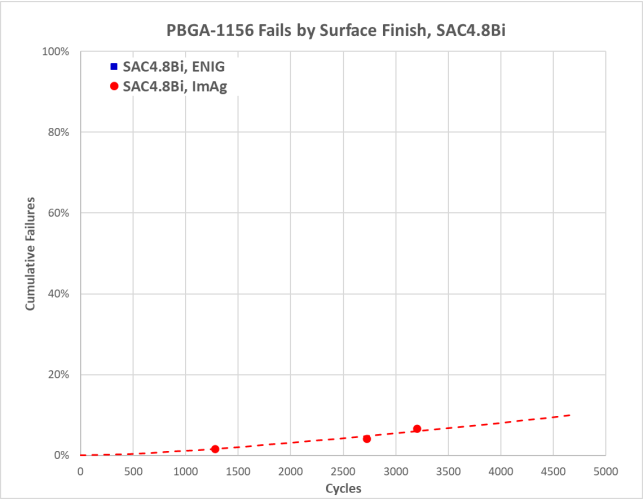

App Figure 5: PBGA-1156 SAC4.8Bi ENIG vs. ImAg, All Fails

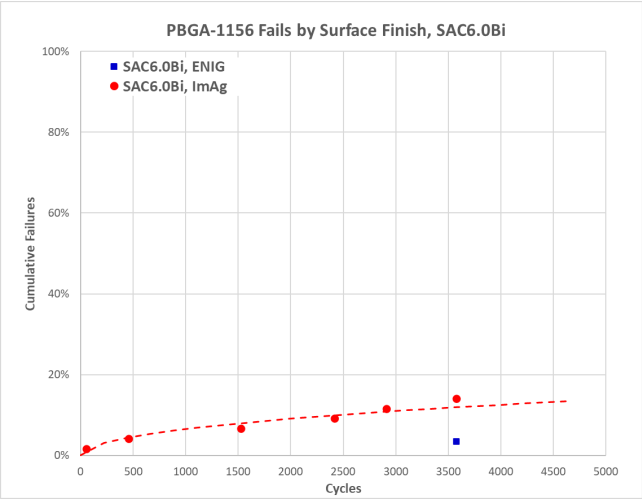

App Figure 6: PBGA-1156 SAC4.8Bi ENIG vs. ImAg, All Fails

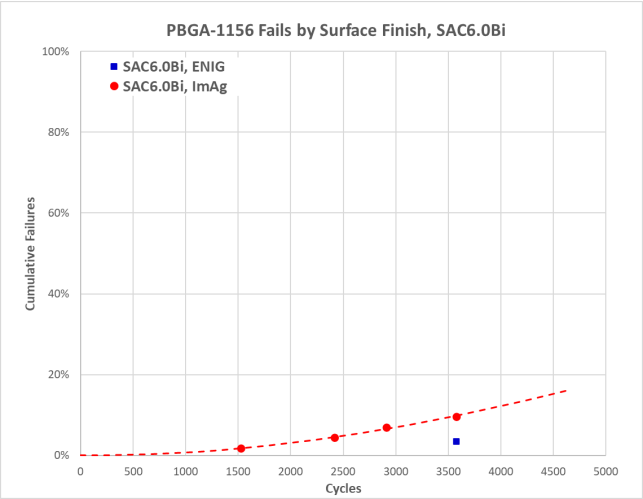

App Figure 7: PBGA-1156 SAC6.0Bi ENIG vs. ImAg, No Outliers

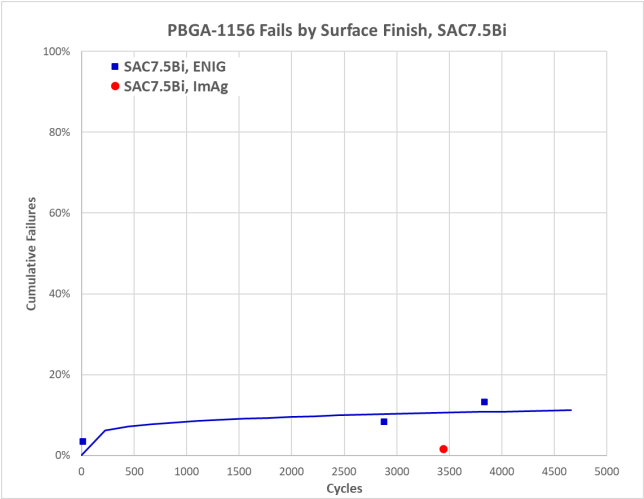

App Figure 8: PBGA-1156 SAC7.5Bi ENIG vs. ImAg, All Fails

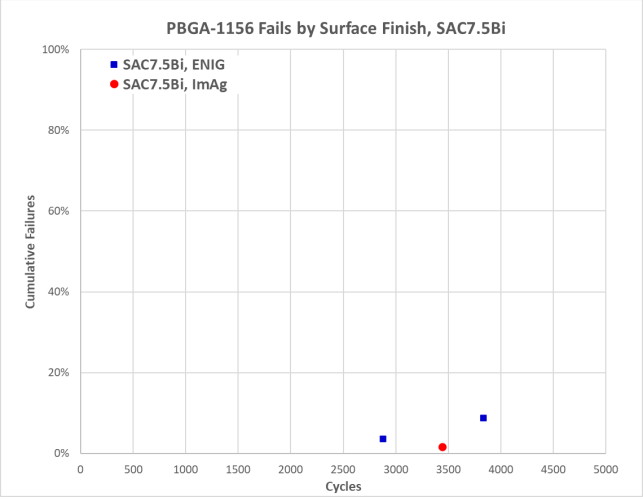

App Figure 9: PBGA-1156 SAC7.5Bi ENIG vs. ImAg, No Outliers

PBGA-676

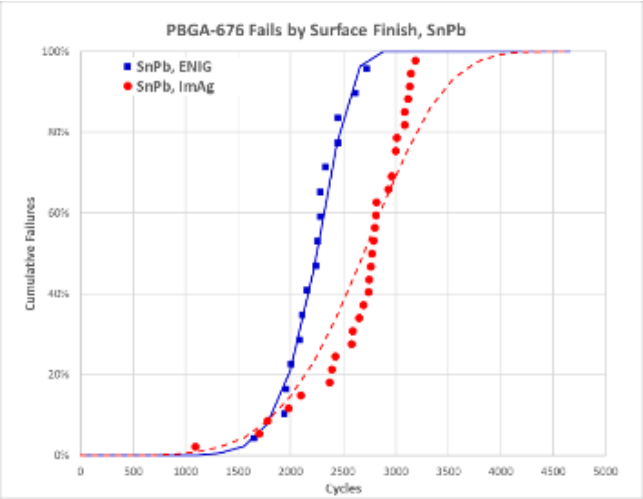

App Figure 10: PBGA-676 SnPb ENIG vs. ImAg, All Fails

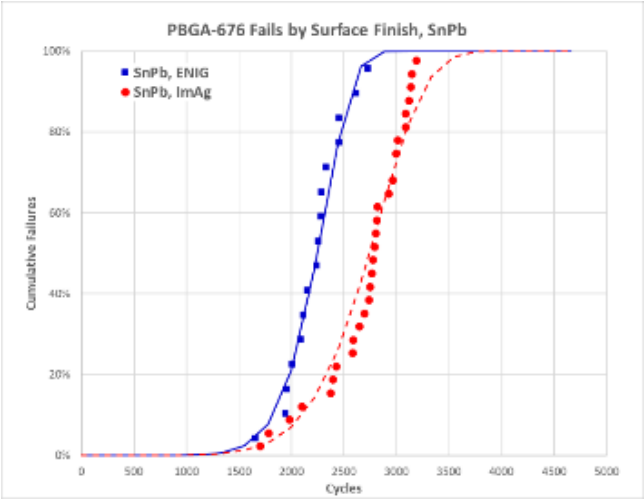

App Figure 11: PBGA-676 SnPb ENIG vs. ImAg, No Outliers

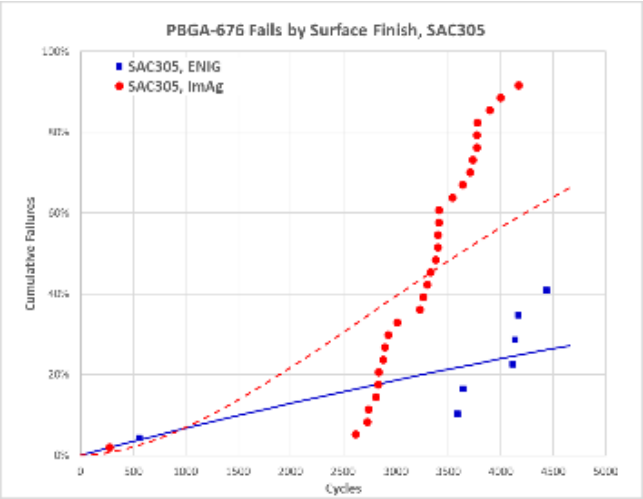

App Figure 12: PBGA-676 SAC305 ENIG vs. ImAg, All Fails

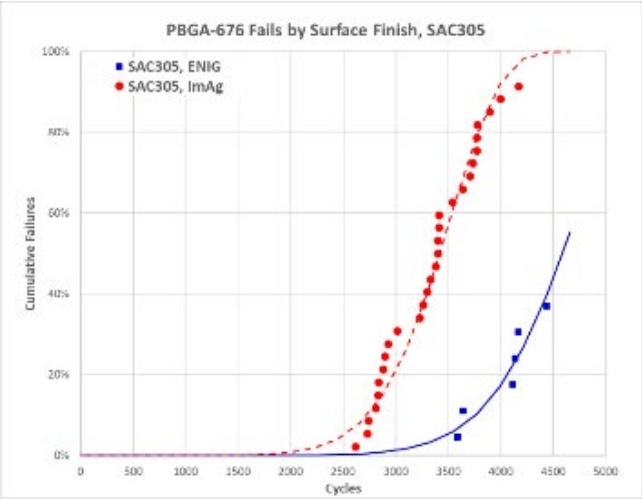

App Figure 13: PBGA-676 SAC305 ENIG vs. ImAg, No Outliers

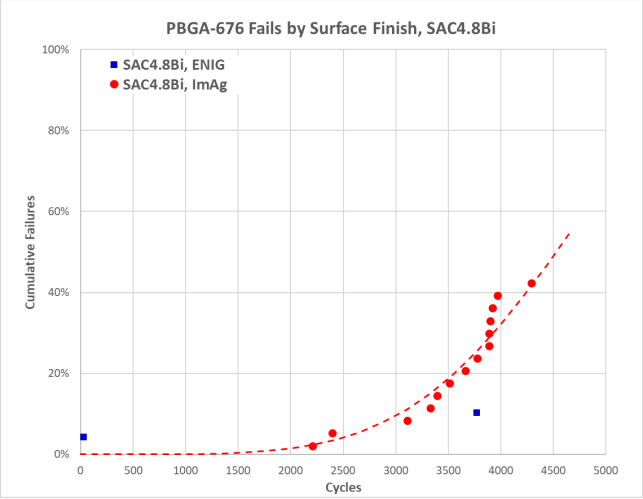

App Figure 14: PBGA-676 SAC4.8Bi ENIG vs. ImAg, All Fails

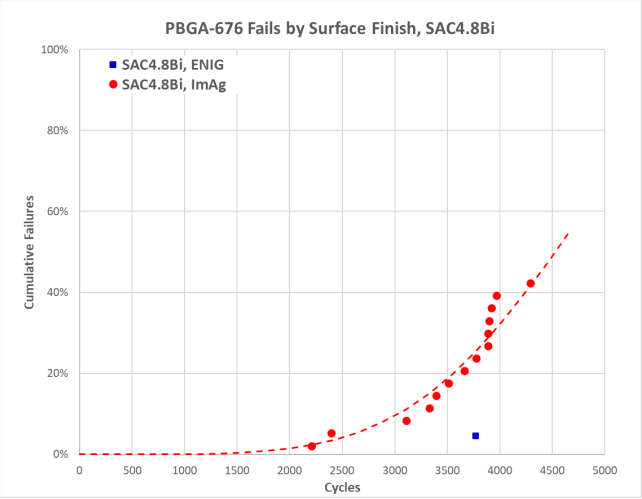

App Figure 15: PBGA-676 SAC4.8 ENIG vs. ImAg, No Outliers

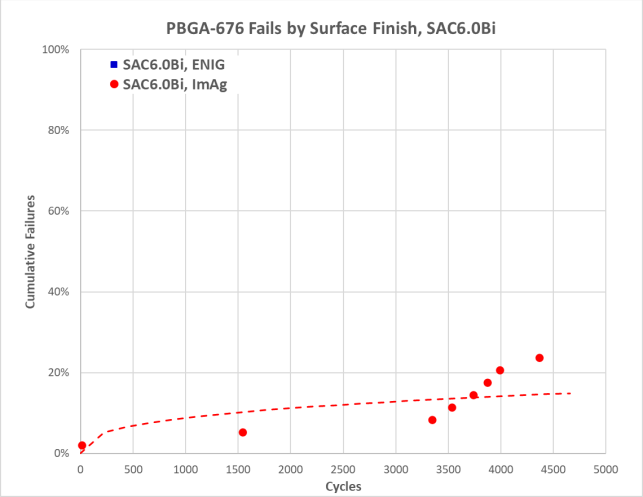

App Figure 16: PBGA-676 SAC6.0Bi ENIG vs. ImAg, All Fails

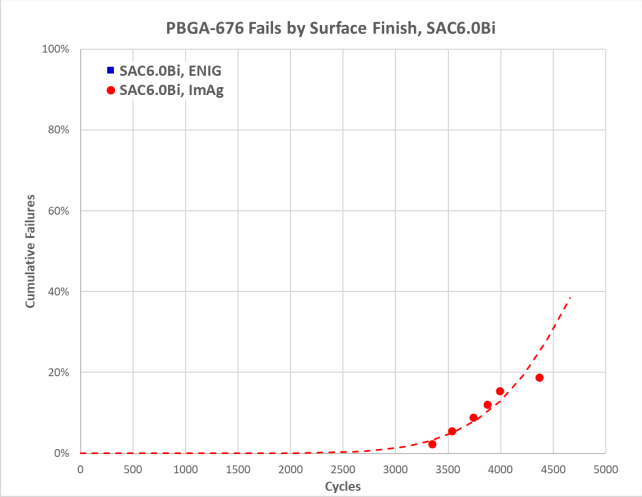

App Figure 17: PBGA-676 SAC6.0Bi ENIG vs. ImAg, No Outliers

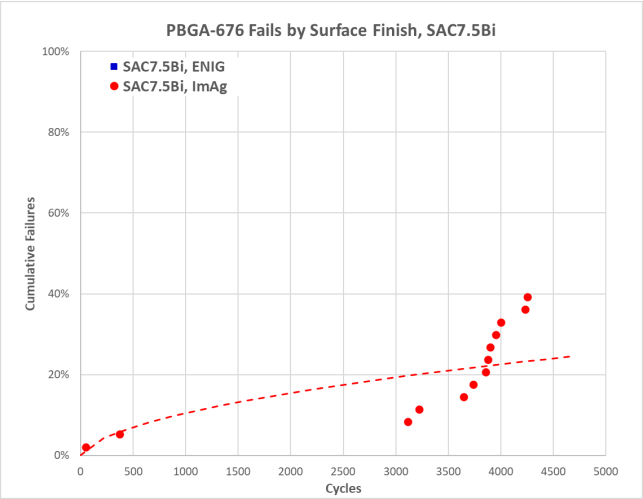

App Figure 18: PBGA-676 SAC7.5Bi ENIG vs. ImAg, All Fails

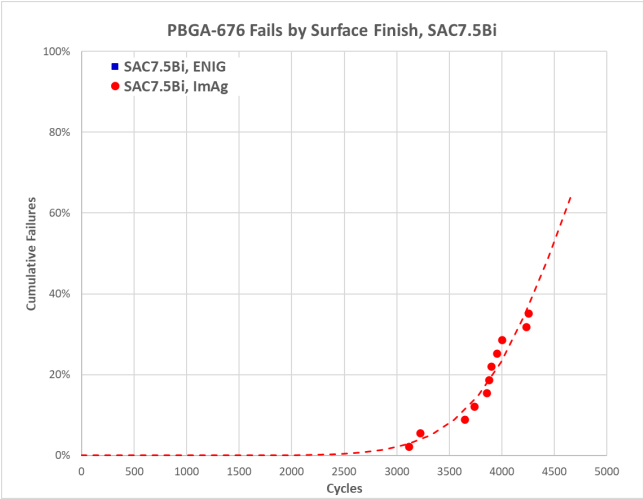

App Figure 19: PBGA-676 SAC7.5Bi ENIG vs. ImAg, No Outliers

CLCC-20

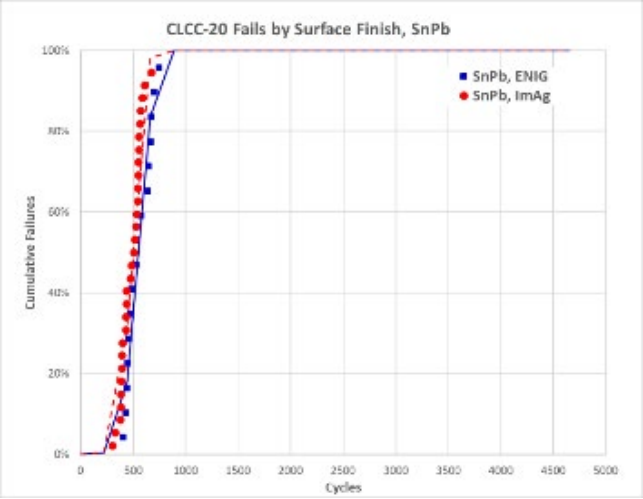

App Figure 20: CLCC-20 SnPb ENIG vs. ImAg, All Fails

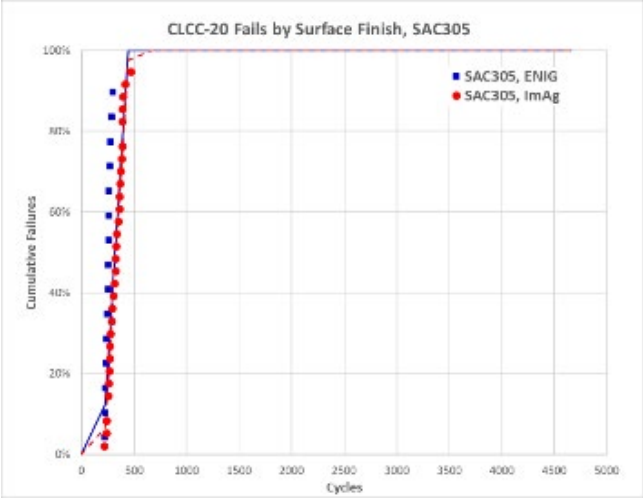

App Figure 21: CLCC-20 SAC305 ENIG vs. ImAg, All Fails

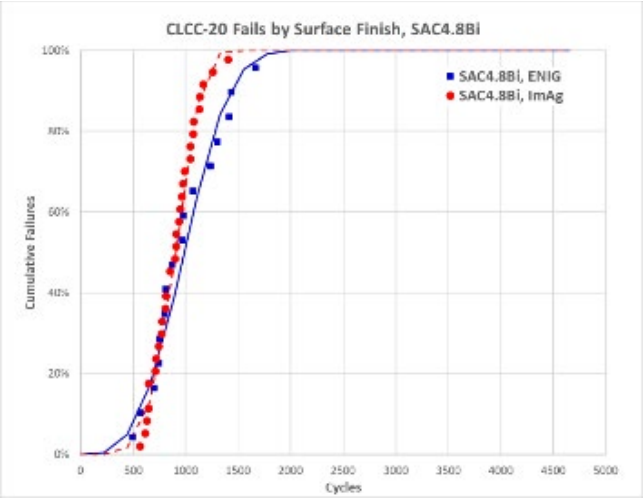

App Figure 22: CLCC-20 SAC4.8Bi ENIG vs. ImAg, All Fails

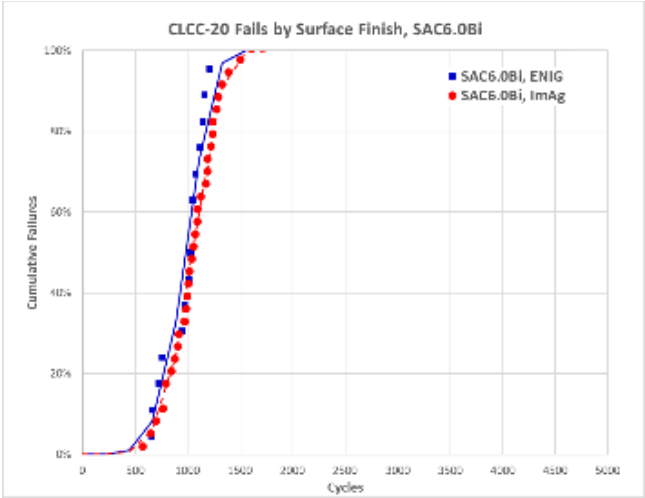

App Figure 23: CLCC-20 SAC6.0Bi ENIG vs. ImAg, All Fails

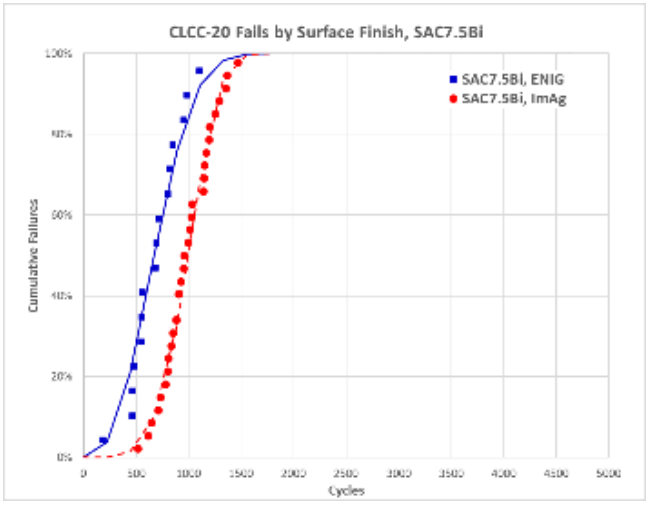

App Figure 24: CLCC-20 SAC7.5Bi ENIG vs. ImAg, All Fails

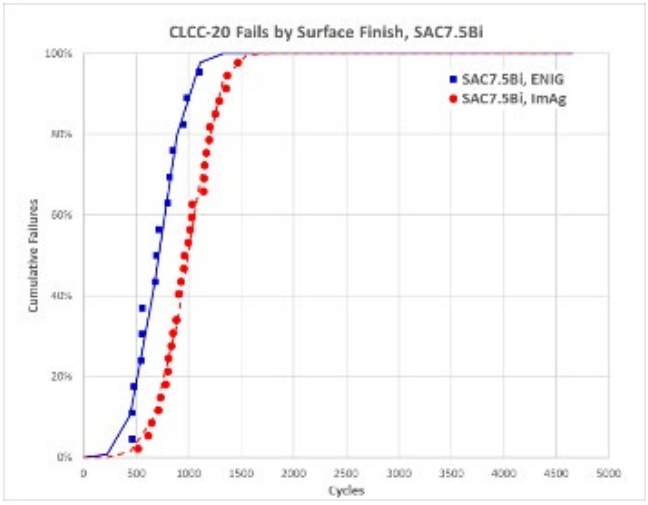

App Figure 25: CLCC-20 SAC7.5Bi ENIG vs. ImAg, No Outliers

MLF-20

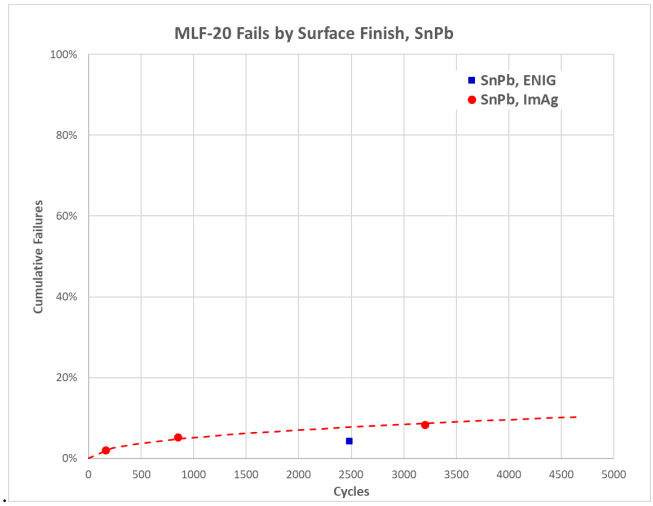

App Figure 26: MLF-20 SnPb ENIG vs. ImAg, All Fails

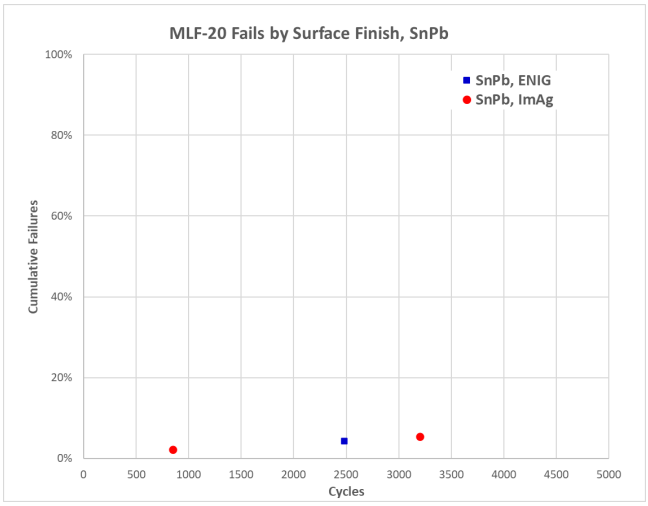

App Figure 27: MLF-20 SnPb ENIG vs. ImAg, No Outliers

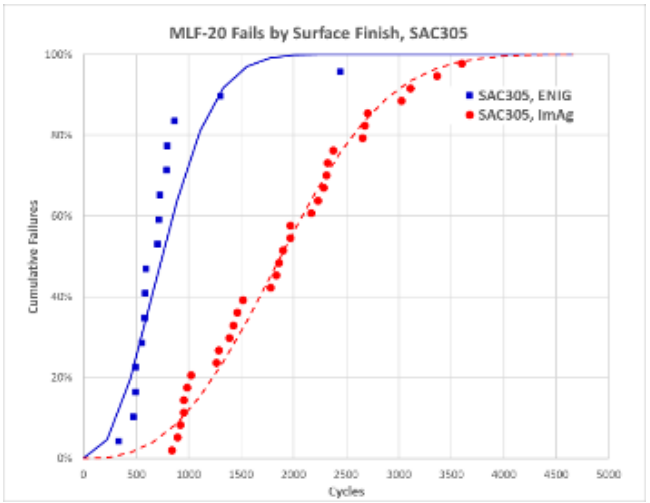

App Figure 28: MLF-20 SAC305 ENIG vs. ImAg, All Fails

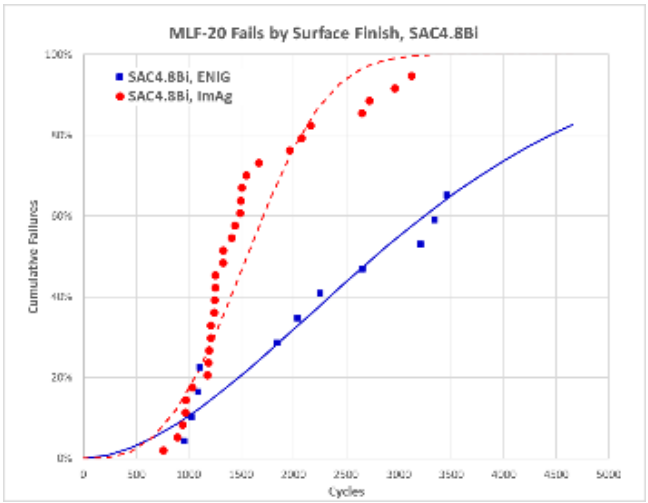

App Figure 29: MLF-20 Sac4.8Bi ENIG vs. ImAg, All Fails

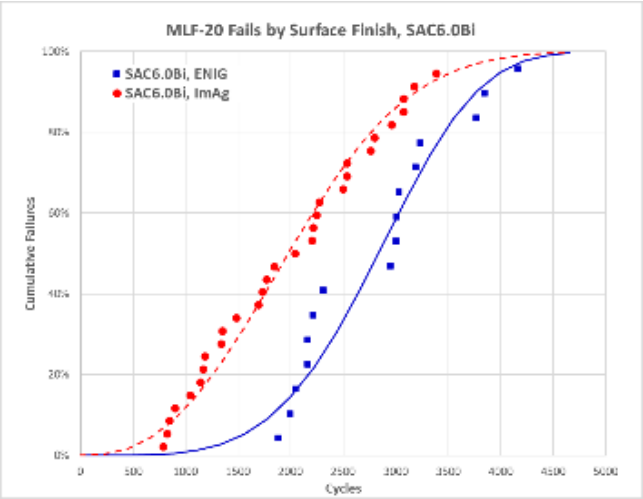

App Figure 30: MLF-20 SAC6.0Bi ENIG vs. ImAg, All Fails

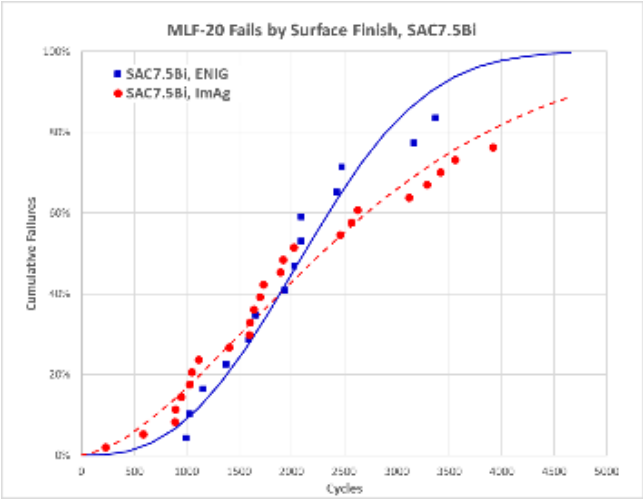

App Figure 31: MLF-20 SAC7.5Bi ENIG vs. ImAg, All Fails

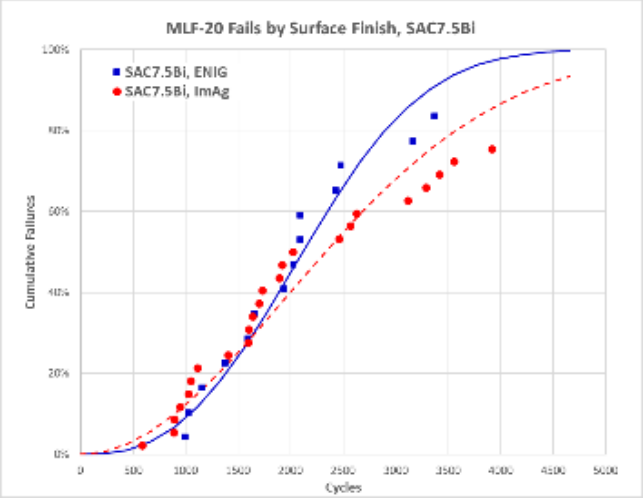

App Figure 32: MLF-20 SAC7.5Bi ENIG vs. ImAg, No Outliers

SOT-23

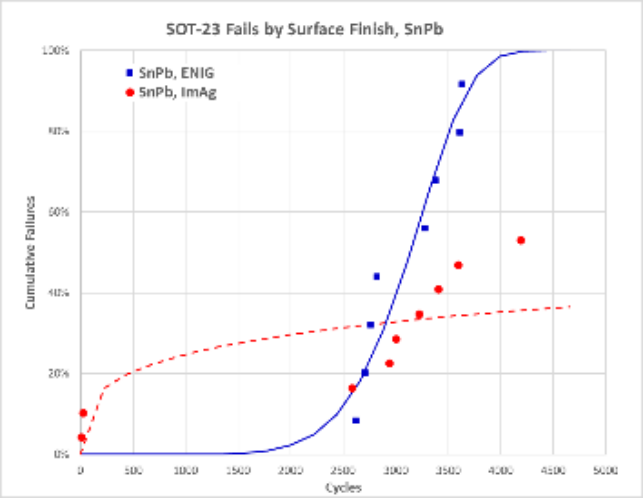

App Figure 33: SOT-23 SnPb ENIG vs. ImAg, All Fails

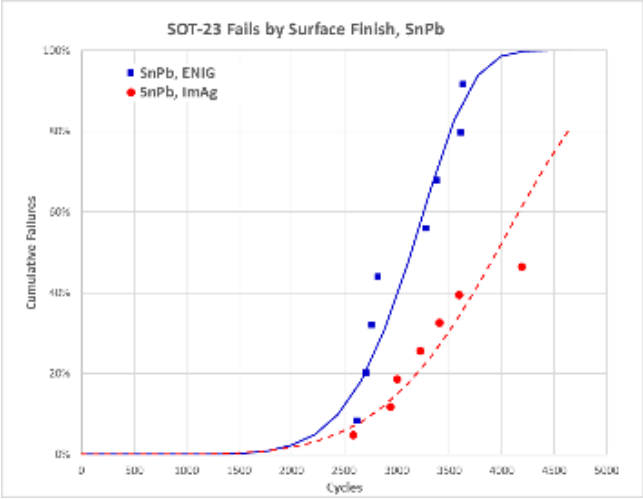

App Figure 34: SOT-23 SnPb ENIG vs. ImAg, No Outliers

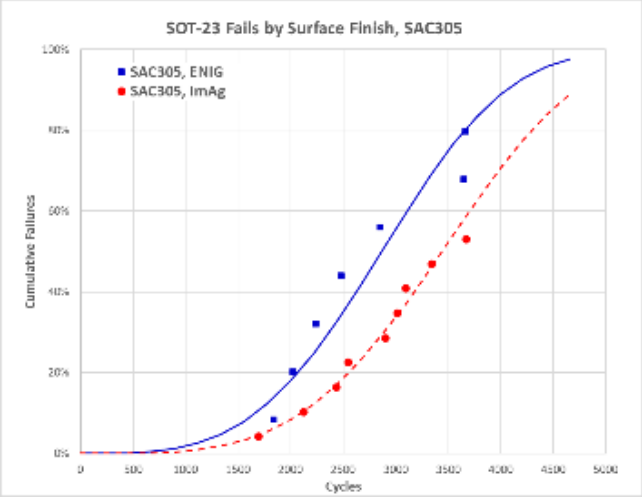

App Figure 35: SOT-23 SAC305 ENIG vs. ImAg, All Fails

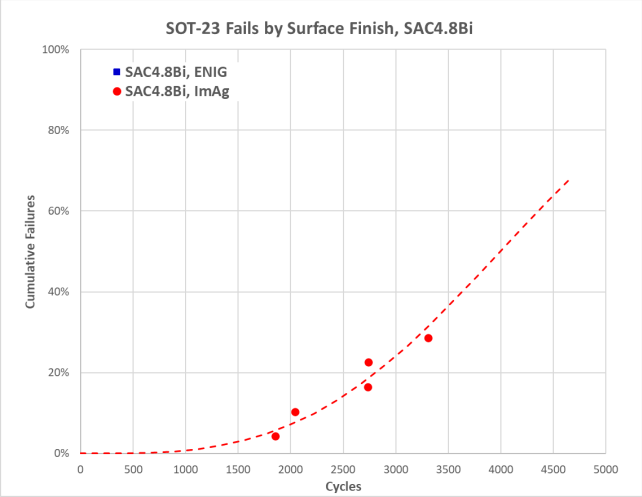

App Figure 36: SOT-23 SAC4.8Bi ENIG vs. ImAg, All Fails

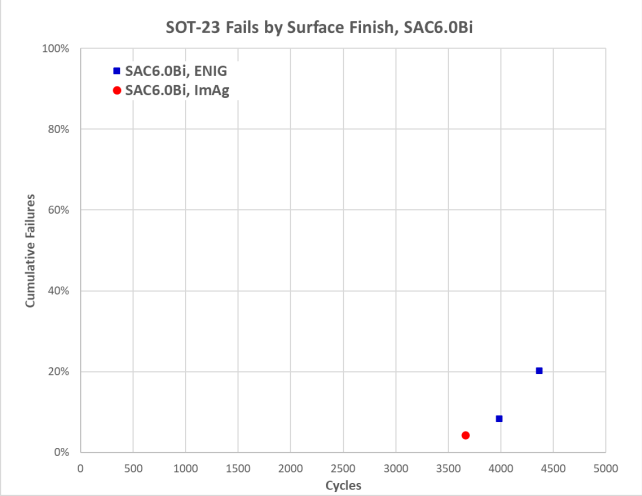

App Figure 37: SOT-23 SAC6.0Bi ENIG vs. ImAg, All Fails

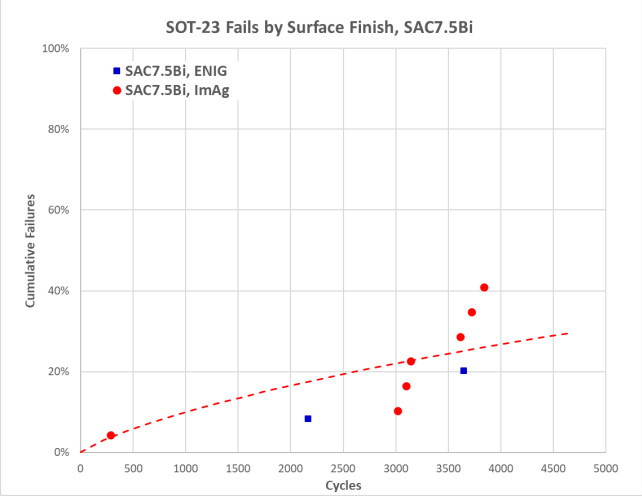

App Figure 38: SOT-23 SAC7.4Bi ENIG vs. ImAg, All Fails

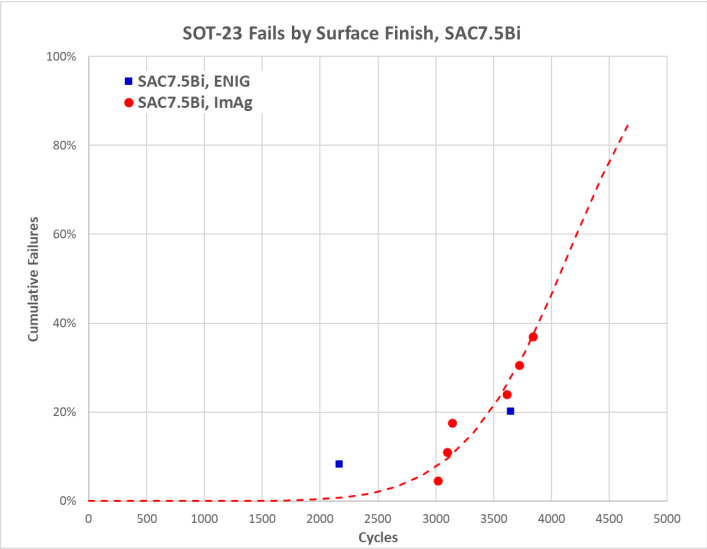

App Figure 39: SOT-23 SAC7.5Bi ENIG vs. ImAg, No Outliers

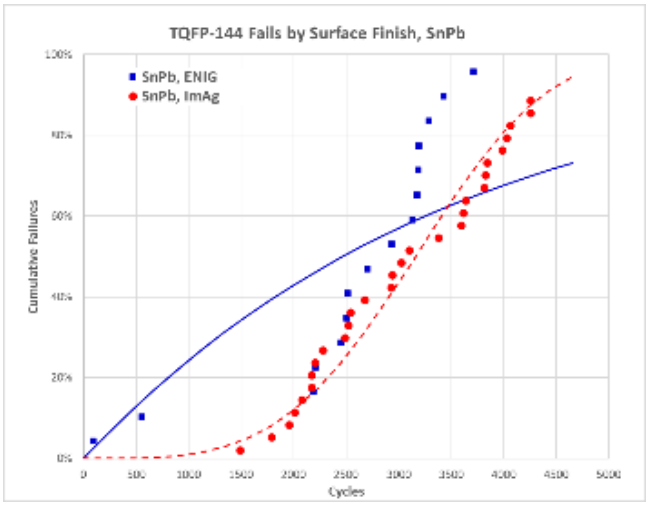

App Figure 40: TQFP-144 SnPb ENIG vs. ImAg, All Fails

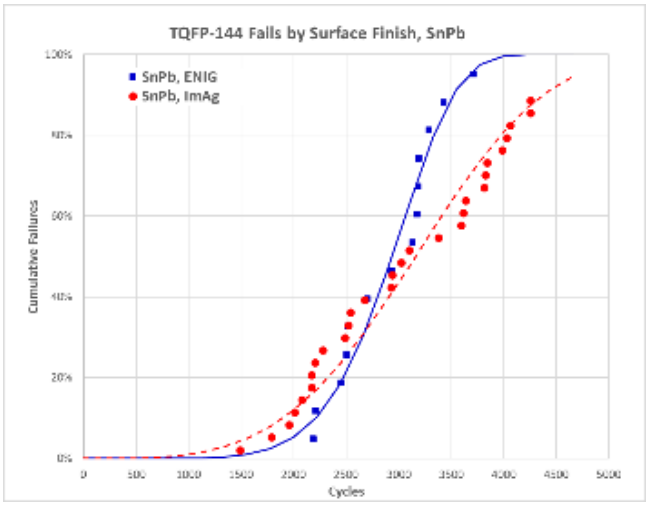

App Figure 41: TQFP-144 SnPb ENIG vs. ImAg, No Outliers

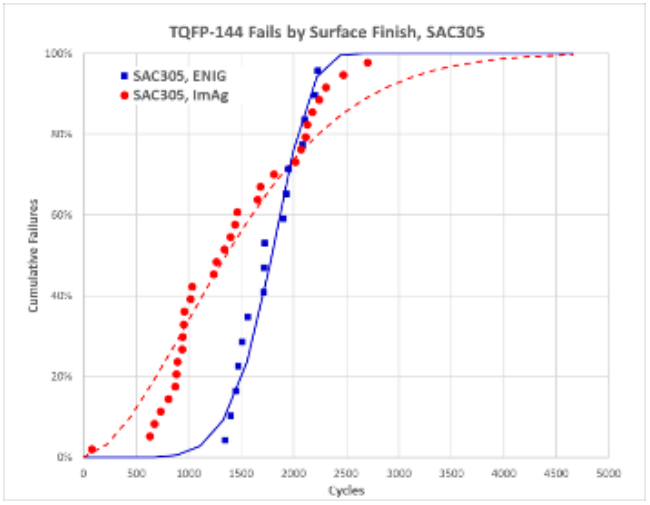

App Figure 42: TQFP-144 SAC305 ENIG vs. ImAg, All Fails

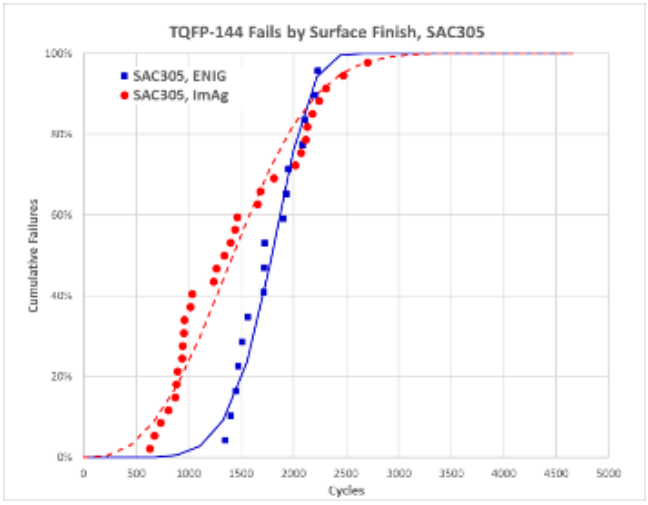

App Figure 43: TQFP-144 SAC305 ENIG vs. ImAg, No Outliers

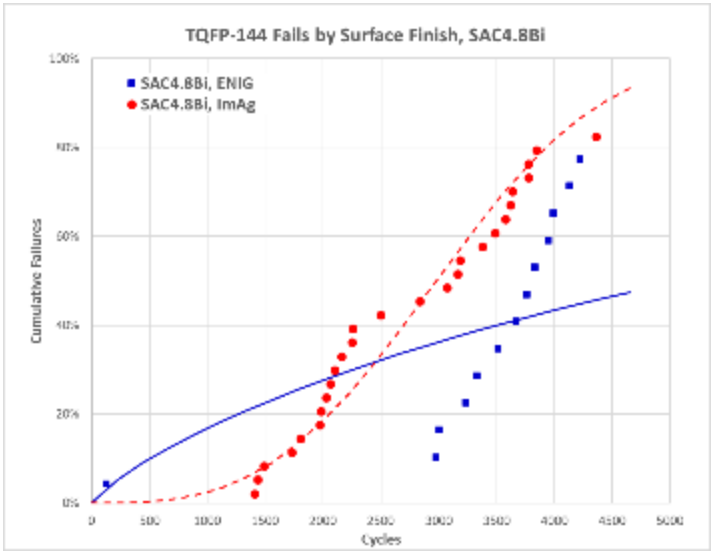

App Figure 44: TQFP-144 SAC4.8Bi ENIG vs. ImAg, All Fails

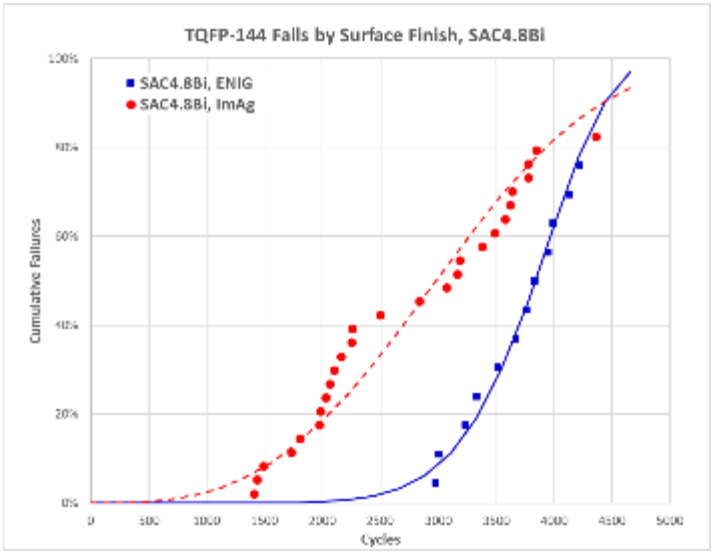

App Figure 45: TQFP-144 SAC4.8Bi ENIG vs. ImAg, No Outliers

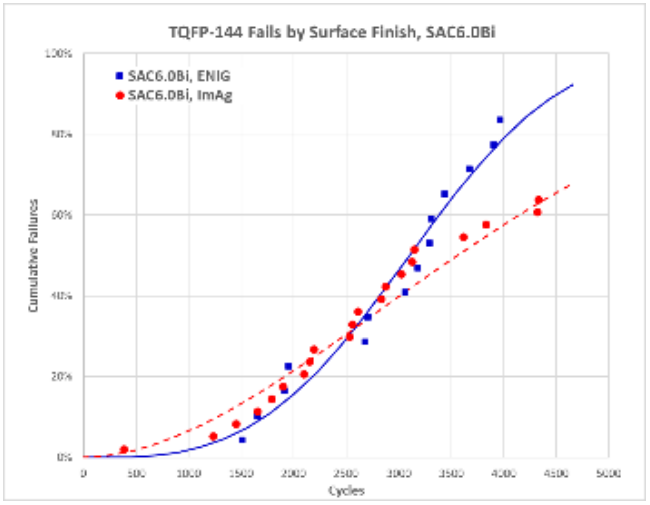

App Figure 46: TQFP-144 SAC6.0Bi ENIG vs. ImAg, All Fails

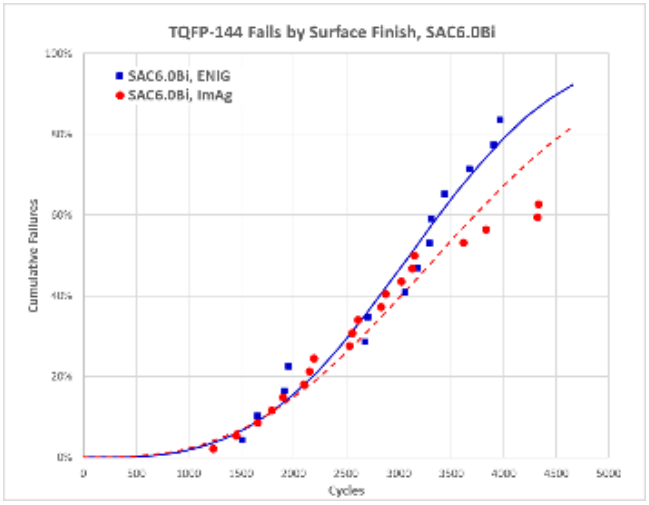

App Figure 47: TQFP-144 SAC6.0Bi ENIG vs. ImAg, No Outliers

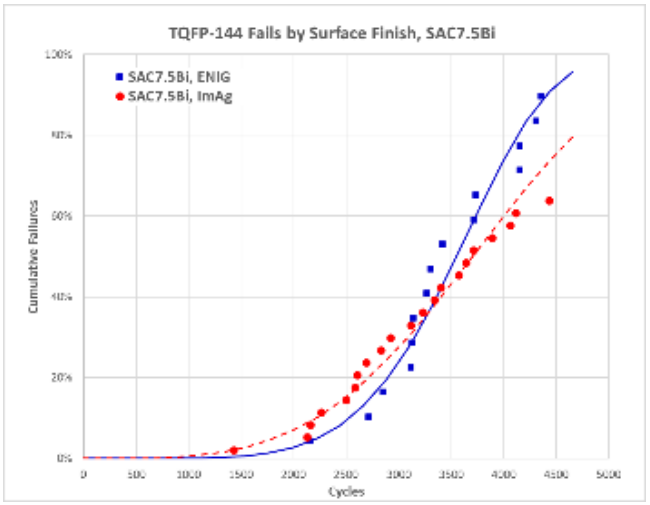

App Figure 48: TQFP-144 SAC7.5Bi ENIG vs. ImAg, All Fails

LGA

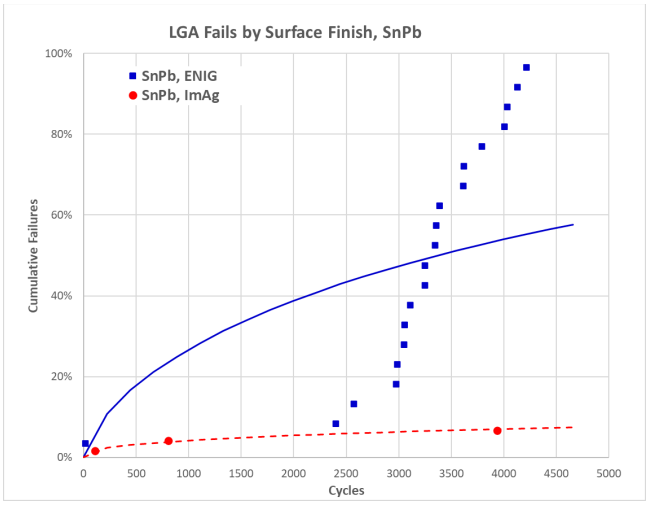

App Figure 49: LGA SnPb ENIG vs. ImAg, All Fails

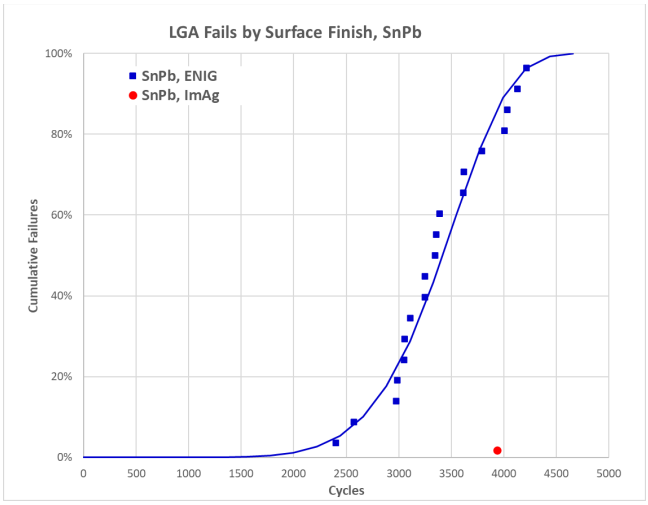

App Figure 50: LGA SnPb ENIG vs. ImAg, No Outliers

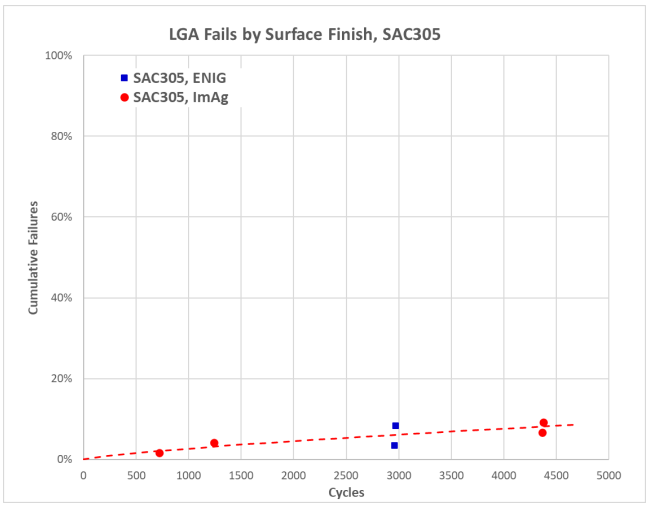

App Figure 51: LGA SAC305 ENIG vs. ImAg, All Fails

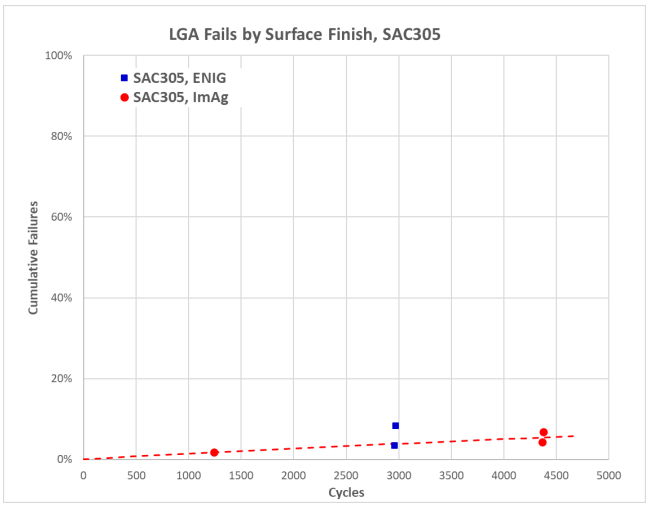

App Figure 52: LGA SAC305 ENIG vs. ImAg, No Outliers

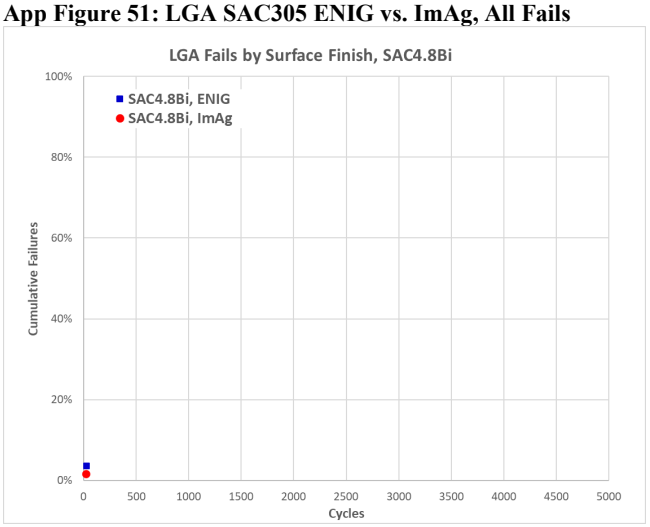

App Figure 53: LGA SAC4.8Bi ENIG vs. ImAg, All Fails

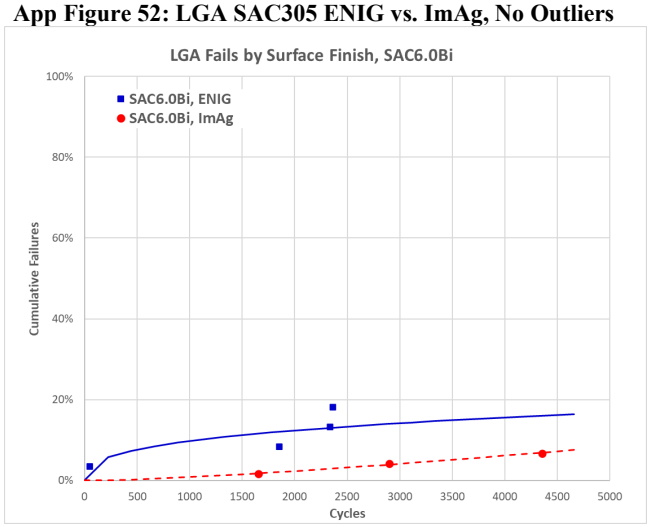

App Figure 54: LGA SAC6.0Bi ENIG vs. ImAg, All Fails

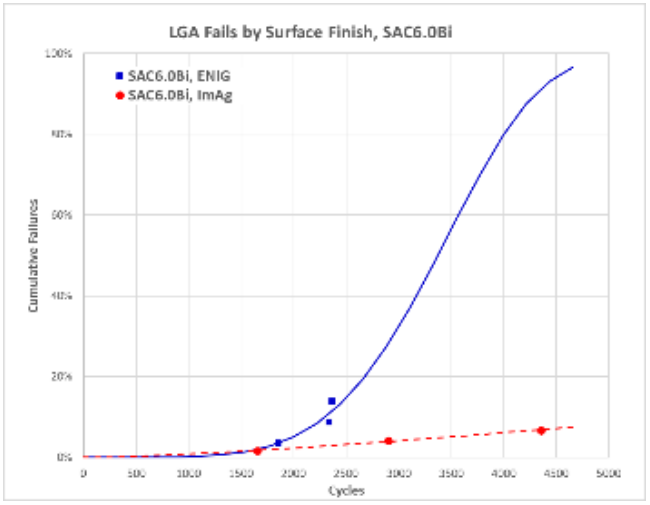

App Figure 55: LGA SAC6.0Bi ENIG vs. ImAg, No Outliers

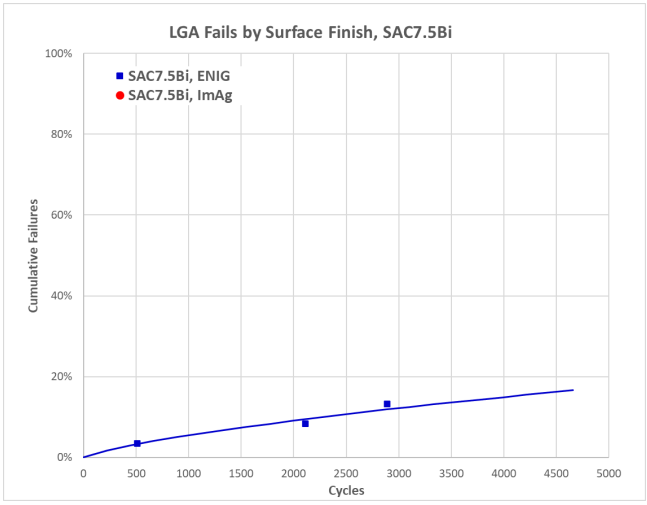

App Figure 56: LGA SAC7.5Bi ENIG vs. ImAg, All Fails

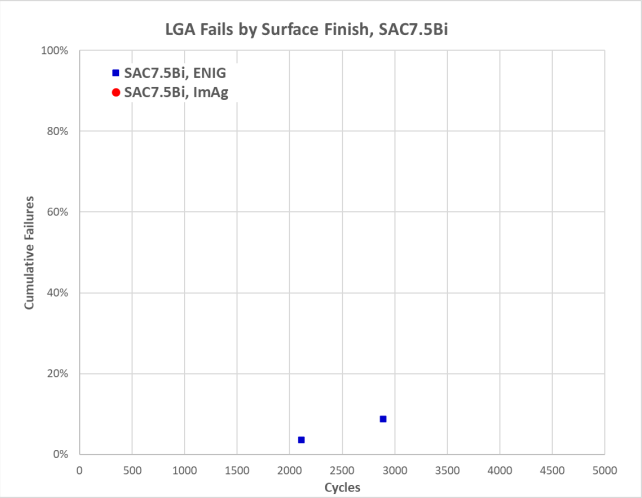

App Figure 57: LGA SAC7.5Bi ENIG vs. ImAg, No Outliers

Appendix D Component Mechanical Information

A-MLF20-5mm-.65mm-DC-(Sn)-TR

Finish: Sn
Mass: 70.10 mg
CTE: Alpha 1= 12.95 µm/(m·°C)
Alpha 2= 20.28 µm/(m·°C)
Tg= 88.49 °C
Sections Over-plated: No

Feature	Symbol	English (mil.)	Metric (mm)
Package Width	PW	196.85	5.00 ± 0.10
Body Width	BW	196.85	5.00 ± 0.10
Package Length	PL	196.85	5.00 ± 0.10
Pitch	P	25.59	0.65 ± 0.05
Lead Width	LW	11.81	0.30 ± 0.05
Lead Length	LL	15.75	0.40 ± 0.05
Lead Thickness	LT	7.87	0.20 ± 0.05
Offset	O	40.50	1.14
Package Thickness	PT	35.43	0.90 ± 0.05
Body Thickness	BT	33.46	0.85 ± 0.05
Die Thickness	-	12.01	0.305
Die Width	DW	125.98	3.20 ± 0.05
Die Length	DL	125.98	3.20 ± 0.05

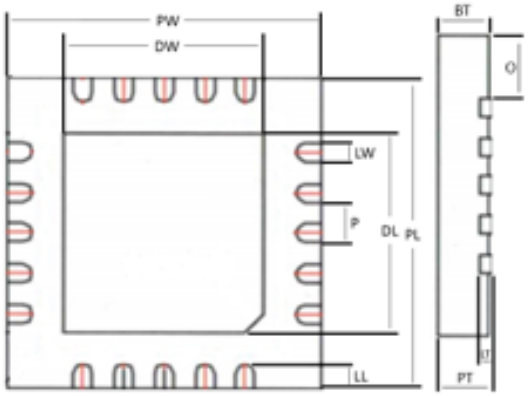

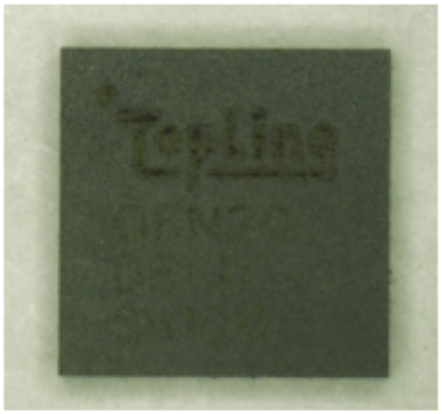

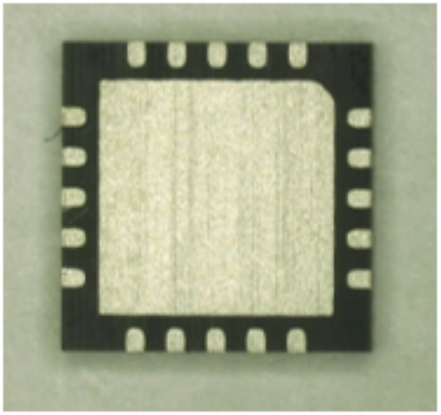

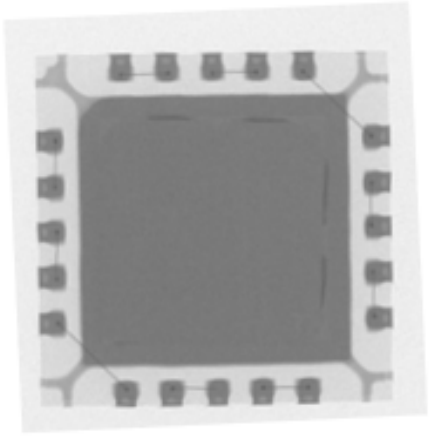

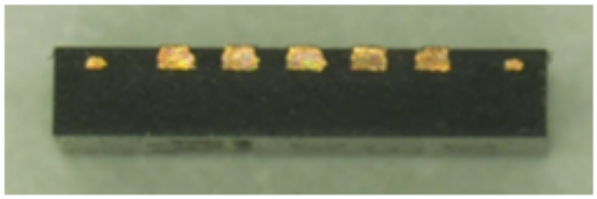

SOT23TR-DC123-Sn

Finish: Sn
Mass: 8.00 mg
CTE: 29.7
Sections Over-plated: No

Feature	Symbol	English (in.)	Metric (mm)
Package Width	PW	94.49 mil	2.40 ± 0.30
Body Width	W	51.18 mil	$1.30^{+0.20}_{-015}$
Package Length	L	114.96 mil	2.92 ± 0.20
Pitch	P	74.80 mil	1.90 ± 0.03
Lead Width	LW	14.57-23.62 mil	0.37-0.60 Min/Max
Lead Length	LL	21.65 mil	0.55 ± 0.03
Offset (1,2)	O1, O2	49.21, 11.42 mil	1.25, 0.29
Package Thickness	PT	43.31 mil	1.10 ± 0.3 Max
Body Thickness	BT	36.61 mil	0.93 ± 0.03
Leg	Leg	11.20 mil	0.28
Knee	Knee	9.50 mil	0.24
Foot	Foot	14.00 mil	0.36

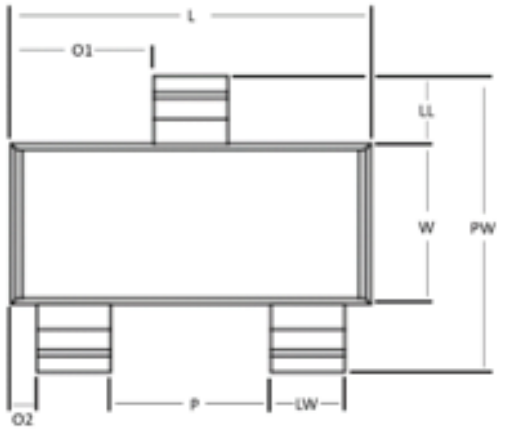

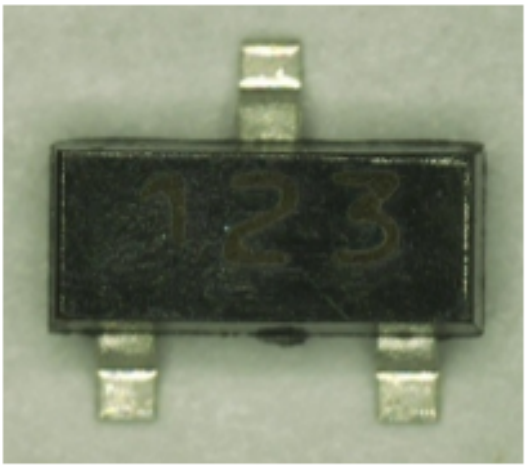

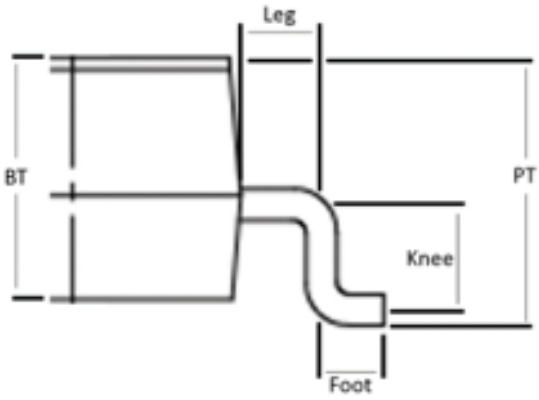

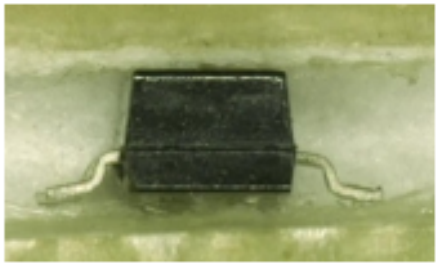

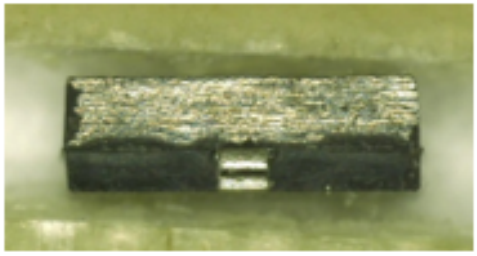

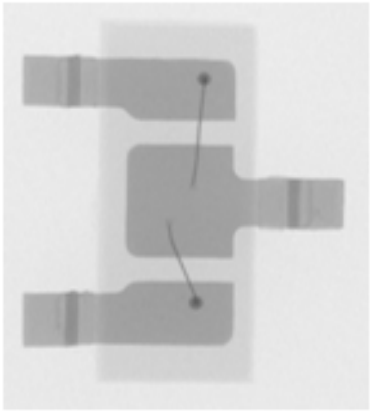

A-PBGA676-1.0mm-27mm-DC

Finish: Sn63 or SAC305
Mass: 2.77 g
CTE: Alpha 1= 18.96 µm/(m·°C)
Sections Over-plated: No

Feature	Symbol	English (in.)	Metric (mm)
Package Width	PW	1.06	27.00
Body Width	BW	0.94	$24.00^{+0.35}_{-0.05}$
Package Length	PL	1.06	27.00
Pitch	P	39.37 mil	1.00
Package Thickness	PT	88.58 mil	2.25
Body Thickness	BT	45.29 mil	1.15
Die Thickness	-	0.014	0.35
Die Width	-	0.67	17.00
Die Length	-	0.67	17.00

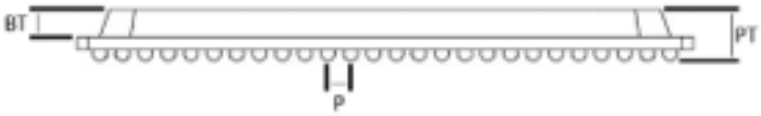

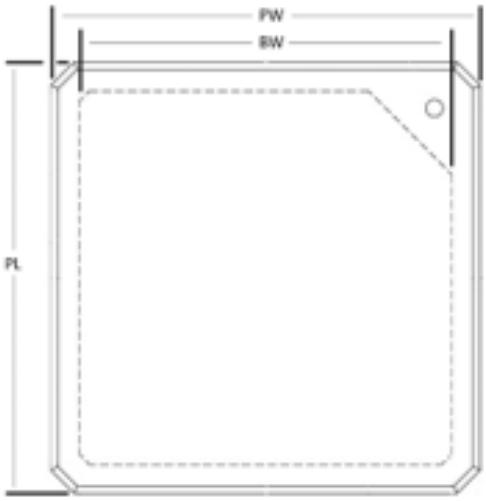

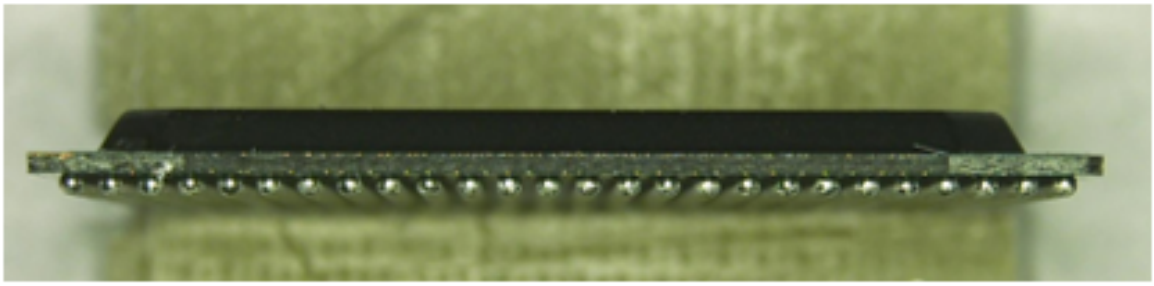

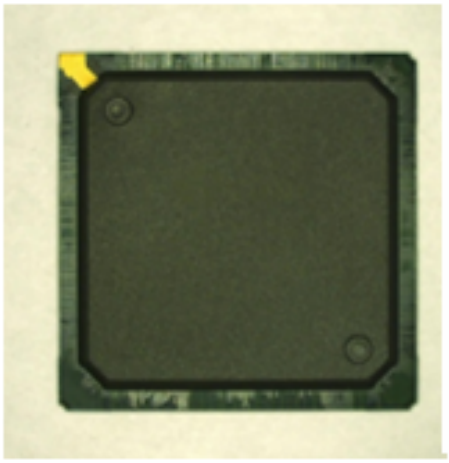

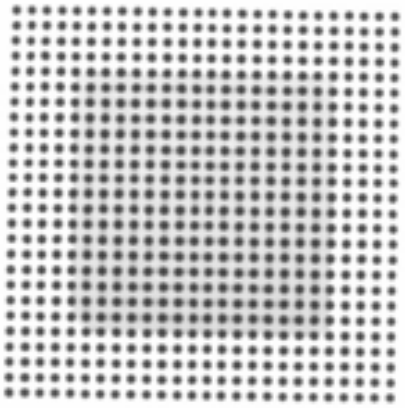

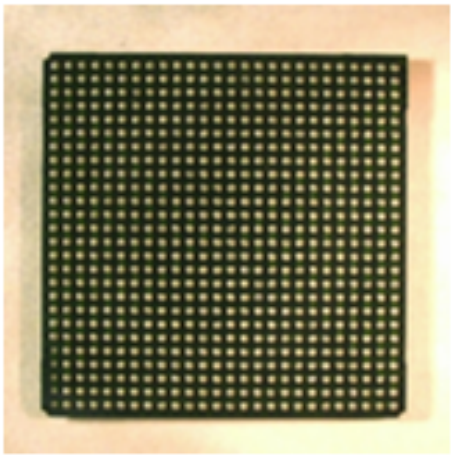

A-TQFP144-20mm-.5-2.0-DC-Sn

Finish: Sn
Mass: 1.01 g
CTE: Alpha 1=13.63 µm/(m·°C)
Alpha 2= 23.85 µm/(m·°C)
Tg= 85.22 °C
Sections Over-plated: No

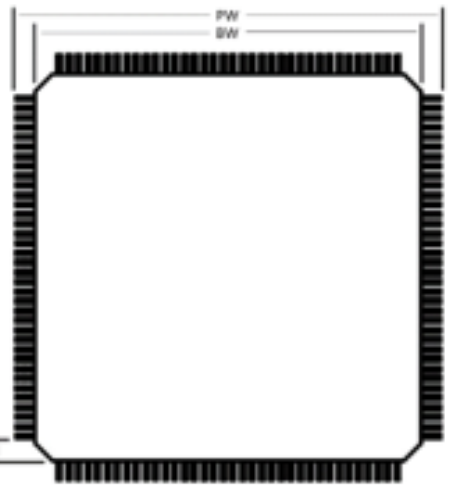

Feature	Symbol	English (mil.)	Metric (mm)
Package Width	PW	866.14	22.00
Body Width	BW	787.40	20.00
Package Length	PL	866.14	22.00
Pitch	P	19.69	0.50
Lead Width	LW	8.66	0.22
Offset	O	39.37	1.00
Package Thickness	PT	39.37	1.00
Body Thickness	BT	39.37	1.00
Leg	Leg	13.78	0.35
Foot	Foot	17.72	0.45
Knee	Knee	15.75	0.40
Die Thickness	-	5.51	0.14
Die Width	-	204.72	5.20
Die Length	-	204.72	5.20

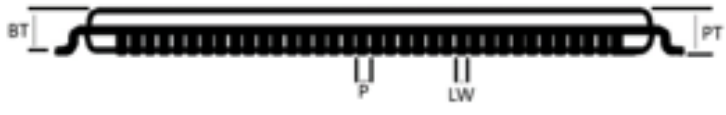

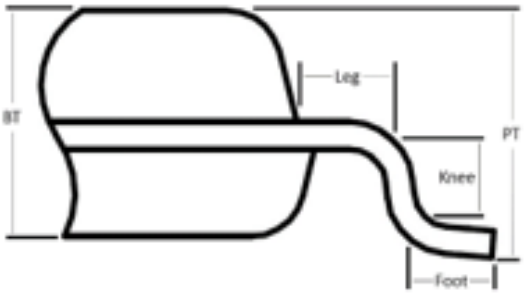

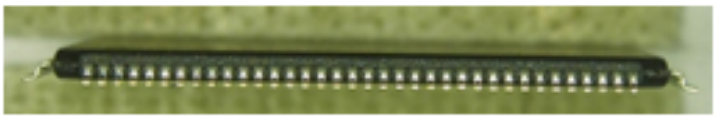

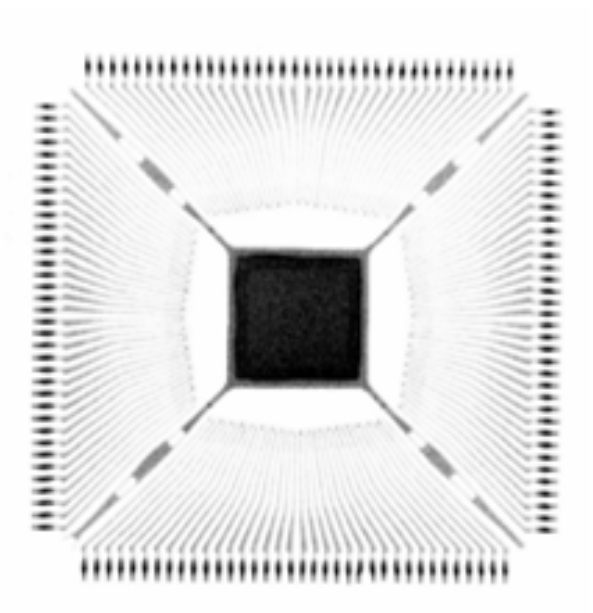

A-PBGA1156-1.0mm-35mm-DC

Finish: Sn63 or SAC305

Mass: 4.83 g

CTE: Alpha 1= 15.81 µm/(m·°C) Alpha 2 = 10.17 µm/(m·°C)

Tg= 186.38 °C

Sections Over-plated: No

Feature	Symbol	English (in.)	Metric (mm)
Package Width	PW	1.38	35.00
Body Width	BW	1.18	30.00
Package Length	PL	1.38	35.00
Pitch	P	39.37 mil	1.00
Package Thickness	PT	88.58 mil	2.25
Body Thickness	BT	46.06 mil	1.17 ± 0.05
Die Thickness	DT	27.50 mil	0.70
Die Width	DW	610.24 mil	15.50
Die Length	DL	610.24 mil	15.50

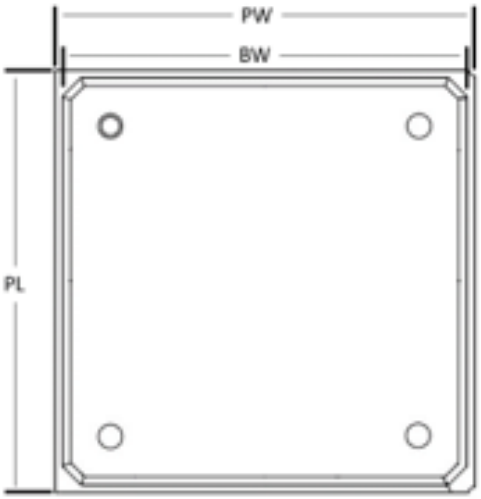

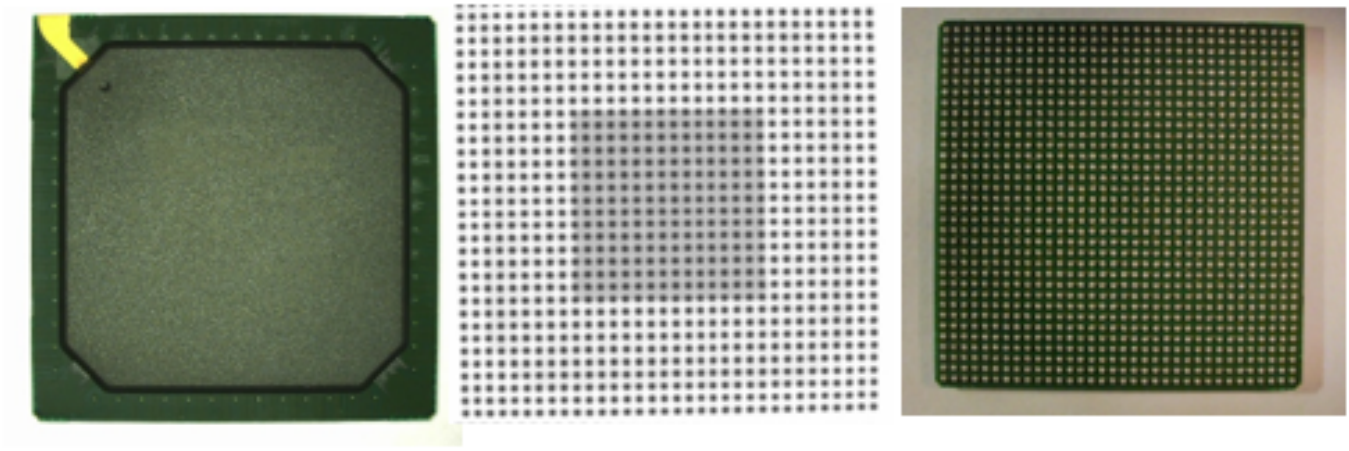

20LCC-1.27mm-8.90mm-DC-L-TR

Finish:
Mass: 0.47 g
CTE: 6.7 ppm
Sections Over-plated: No

Feature	Symbol	English (in.)	Metric (mm)
Package Width	PW	0.35	8.90
Body Width	BW	0.30	7.50
Package Length	PL	$0.35^{+0.01}_{-0.05}$	8.90
Pitch	P	50.00 mil	1.27
Lead Width	LW	25.00 mil	0.40
Pin1 Length	P1L	85.00 mil	2.16
Lead Length	LL	50.00 mil	1.27
Offset	O	63.00 mil	1.60
Package Thickness	PT	75.00 mil	1.94
Body Thickness	BT	60.00 mil	1.52
Plating 1	Ni	80.00 mil	2.03
Plating 2	Au	60.00 mil	1.52
Die Thickness	-	7.87 mil	0.20
Die Width	-	0.16	4.06
Die Length	-	0.16	4.06

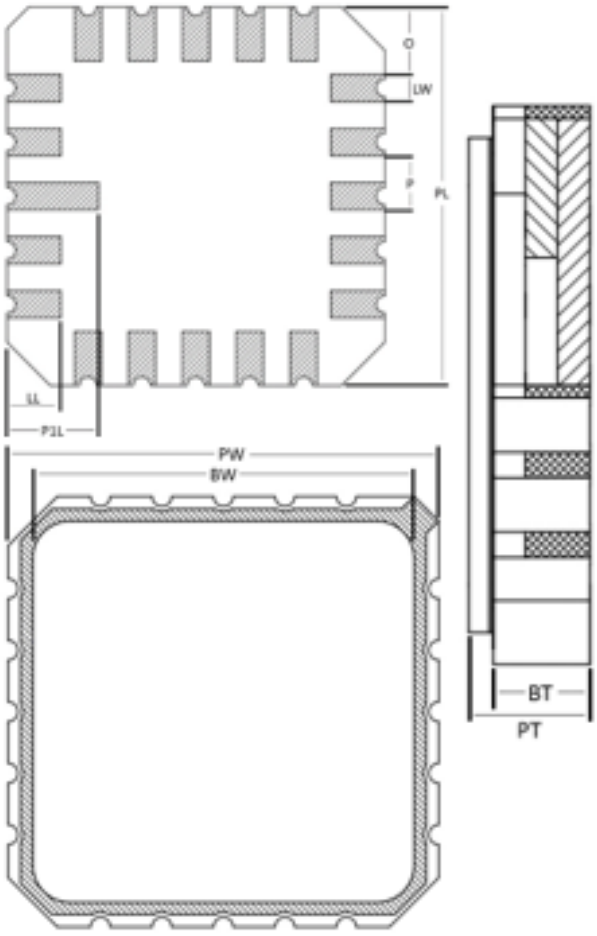

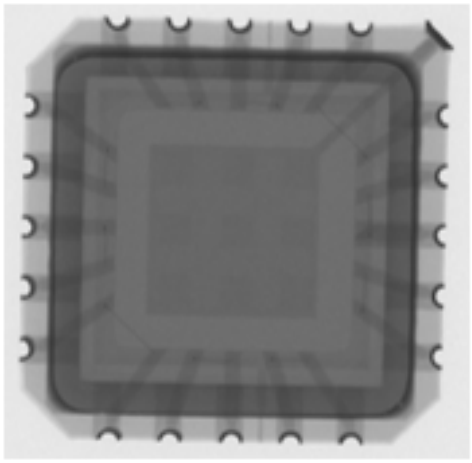

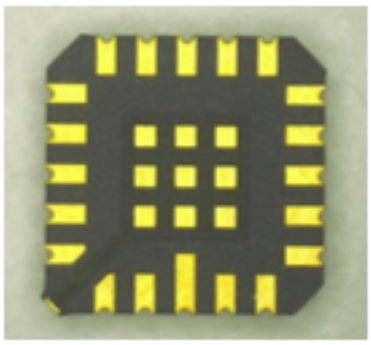

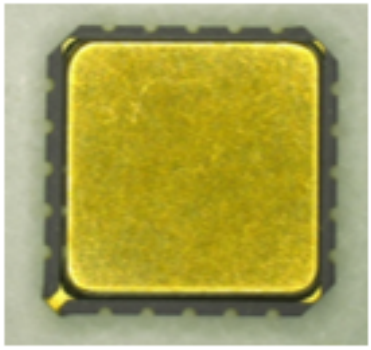

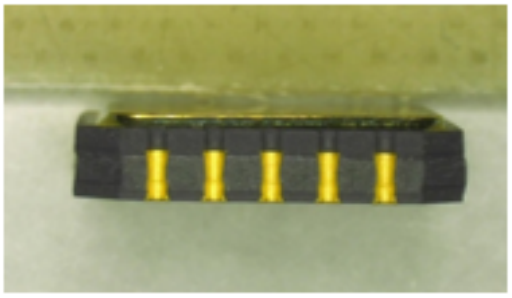

LGA Package

Finish:
Mass: 0.92 g
CTE: 27.9 ppm
Sections Over-plated: No

Feature	Symbol	English (in.)	Metric (mm)
Package Width	PW	0.35	9.00
Package Length	PL	0.44	11.25
Pitch	P	50.00 mil	1.27
Lead Width	LW	25.20 mil	0.64 ± 0.03
Offset	O1, O2, O3, O4	34.00, 184.00, 75.00, 14.80 mil	0.86, 4.67, 1.91, 0.38
Package Thickness	PT	0.11	2.82 ± 0.10

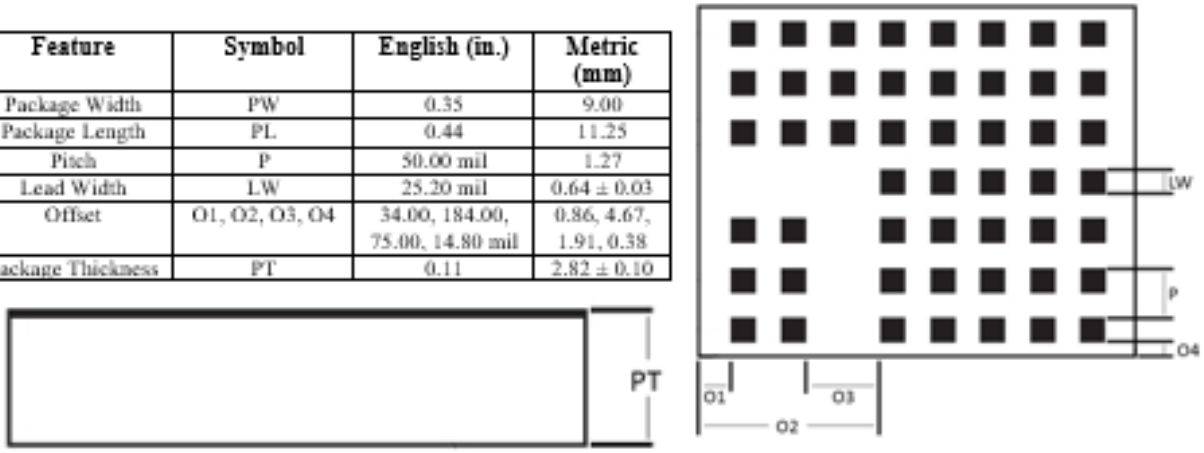

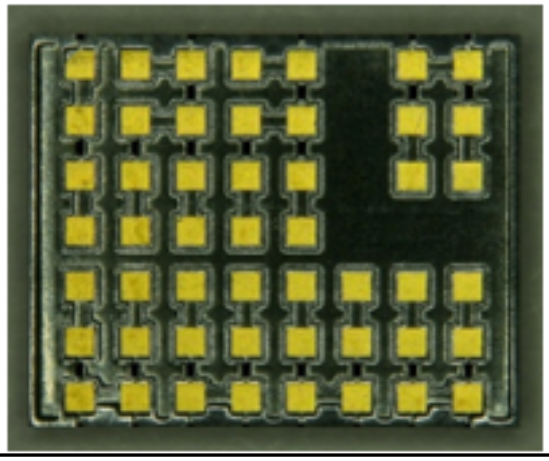

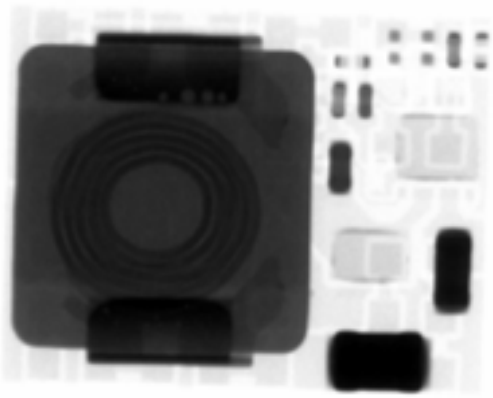

A-PSvfBGA305-.5-12mm-DC-LF-305

Finish:
Mass: 0.20 g
CTE:
Sections Over-plated: No

Feature	Symbol	English (in.)	Metric (mm)
Package Width	PW	0.47	12.00 ± 1.00
Body Width	BW	0.35	9.00
Package Length	PL	0.47	12.00 ± 1.00
Pitch(P1, P2)	P1, P2	25.59, 19.69 mil	0.65, 0.50
Ball Radius	BR	11.81 mil	0.30 ± 0.05
Offset	O	18.70 mil	0.475
Package Thickness	PT	32.68 mil	0.83
Body Thickness	BT	23.62 mil	0.60
Die Thickness	-	6.88 mil	0.17
Die Width	-	257.13 mil	6.53
Die Length	-	257.13 mil	6.53

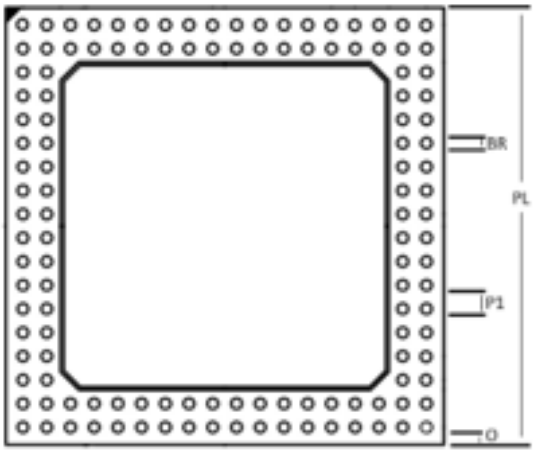

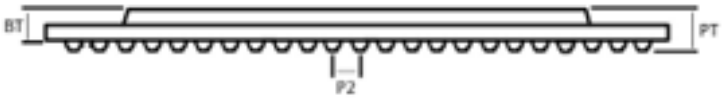

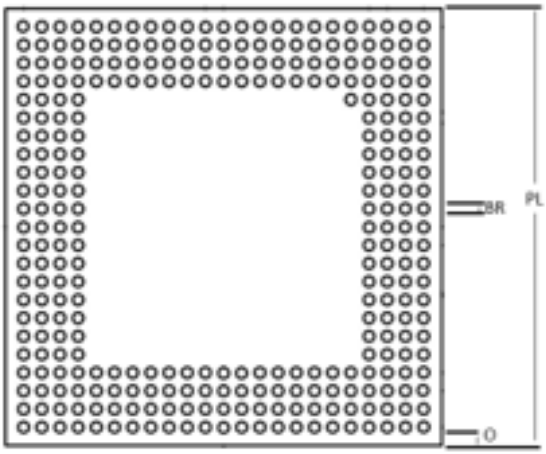

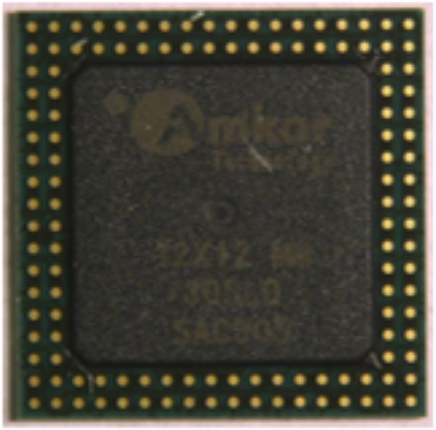

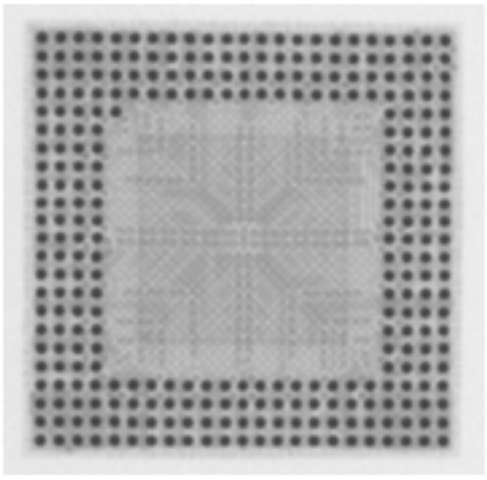

A-PoP128-.65mm-12mm-DC-LF-305

Finish:
Mass: 0.24 g
CTE:
Sections Over-plated: No

Feature	Symbol	English (in.)	Metric (mm)
Package Width	PW	0.47	12.00
Body Width	BW	0.47	12.00
Package Length	PL	0.47	12.00
Pitch	P	25.59, 19.69 mil	0.65, 0.50
Ball Radius	BR	17.72 mil	0.45 ± 0.05
Offset	O	18.70 mil	0.475
Package Thickness	PT	41.73 mil	1.06 ± 0.10
Body Thickness	BT	25.98 mil	0.66 ± 0.05
Die Top/Bottom Thickness	-	6.88/7.62 mil	0.17/0.19
Die Top/Bottom Width	-	257.13/177.17 mil	6.53/4.50
Die Top/Bottom Length	-	257.13/177.17 mil	6.53/4.50